Mapping the molecular mechanism of GTPases KRAS and RIT1 in lung cancer

Kristin Holmes

A dissertation

submitted in partial fulfillment of the

requirements for the degree of

Doctor of Philosophy

University of Washington

2021

Reading Committee:

Alice Berger, Chair

Jonathan Cooper

Hannele Ruohola-Baker

Program Authorized to Offer Degree:

Molecular and Cellular Biology

University of Washington

Abstract

Mapping the molecular mechanism of GTPases KRAS and RIT1 in lung cancer

Kristin Holmes

Chair of the Supervisory Committee:
Alice Berger, Ph.D.
Genome Sciences

RAS genes are mutated in 30% of human cancers, and RAS genes are amongst the most important oncogenes. KRAS and RIT1 (Ras-like in all tissues) have been identified as cancer drivers in 30% and 2% of lung adenocarcinoma, respectively. RIT1 is traditionally studied using the homology between KRAS to inform functional mutations and effector proteins. Defining mutant KRAS or RIT1-specific signaling and critical effector proteins is important, because targeting RAS effector proteins may provide a therapeutic opportunity.

Recently it has been shown that KRAS forms homodimers, and KRAS homodimers are required for mutant *KRAS*- driven tumorigenesis. Preliminary mass spectrometry data identified NRAS as a KRAS interacting protein, raising the possibility that RAS proteins can heterodimerize. In order to investigate if KRAS and NRAS heterodimerize, I employed the biochemical assays of

size exclusion chromatography and co-immunoprecipitation. Size exclusion chromatography resolved Ras homodimers, confirming the catalytic RAS G-domain has an innate ability to form dimers. Future work in optimizing recombinant protein expression is necessary to distinguish RAS homodimers from putative KRAS/NRAS homodimers. Unfortunately, co-immunoprecipitation cannot detect KRAS homodimers or putative KRAS/NRAS heterodimers. Additionally, loss of NRAS in A549 lung adenocarcinoma cells led to a decrease in proliferation, confirming the functional role of NRAS in mutant KRAS cancer. Continuing to characterize RAS dimers may uncover opportunities to abrogate Ras heterodimers for therapeutic benefit.

Global proteomic profiling was performed in order to identify RIT1 and KRAS specific signaling in lung cancer cells. Mutant RIT1 drives epithelial-to-mesenchymal transition (EMT) similar to mutant KRAS by modulating key EMT genes such as Vimentin, Fibronectin1, N-Cadherin, Keratin19. Interestingly, mutant RIT1 and KRAS induced down-regulation of HLA proteins. Additional work is necessary to elucidate the mechanism of loss of MHC class I complex. Phosphoproteome analysis revealed differential phosphorylation of several EGFR phosphorylation sites. Understanding the similarities and differences in the signaling pathways modulated by mutant RIT1 and mutant KRAS can help to elucidate a therapeutic strategy for RIT1-driven lung adenocarcinoma.

TABLE OF CONTENTS

List of Figures iii

Chapter 1. Introduction 1

1.1 RAS proteins 1

1.2 Ras Regulation 5

1.2.1 RTK/Ras Activation 5

1.2.2 Ras effectors 6

1.2.3 Constitutively active mutations 8

1.3 RAS Dimers 10

1.4 RIT1 Biology 12

1.5 "Ras"-opathy – Noonan Syndrome 18

1.5.1 RAS germline mutations 18

1.5.2 RIT1 germline mutations 19

1.5.3 Treatments 20

1.6 RTK/Ras Signaling in Lung Adenocarcinoma 21

1.6.1 KRAS-driven Lung Adenocarcinoma 22

1.6.2 RIT1-driven Lung Adenocarcinoma 23

1.6.3 Treatment of RAS- and RIT1-driven Lung Adenocarcinoma 25

Chapter 2. NRAS in KRAS-driven lung adenocarcinoma 28

2.1 Introduction 28

2.2 Results 35

2.3 Discussion 51

Chapter 3. Characterizing THE RIT1- and KRAS-REgulated proteome in lung AdenocarcinomA 54

3.1 Introduction 54

3.2 Results 55

3.3 Discussion 70

Chapter 4. Conclusions & Future Direction 73

4.1 Putative KRAS/NRAS heterodimers 73

4.2 Characterizing mutant RIT1 and KRAS proteome in LUAD 75

Chapter 5. Materials and Methods 76

5.1 Plasmids 76

5.2 Cell Line Generation & Proliferation Assay 77

5.3 DNA transfections, Cell Lysis, and Western Blot Analysis 78

5.4 Antibodies/Immunoblotting 78

5.5 Immunoprecipitation 79

5.6 Generating Recombinant Protein Expression Plasmids 79

5.7 Recombinant Protein Expression 80

5.8 Recombinant Protein Purification and Size Exclusion Chromatography 80

Bibliography 84

LIST OF FIGURES

Figure 1.1. Schematic of oncogenic RAS and RIT1 constitutively active signaling..... 2
Figure 1.2. Human wildtype KRAS bound to GDP..... 9
Figure 1.3. Gene expression of RIT1 and RIT2. 15
Figure 2.1. Expression of wildtype and mutant RIT1 and KRAS in AALE epithelial cells32
Figure 2.2. Workflow of LC-MS/MS to identify RIT1 and KRAS specific signaling..... 34
Figure 2.3. Global proteomic profiling data reveals NRAS as a KRAS interactor. 36
Figure 2.4. *NRAS* mRNA expression is downregulated in *KRAS*-mutant lung adenocarcinoma. 39
Figure 2.5. Size exclusion chromatography of his-KRAS^{WT} and his-NRAS^{WT} human recombinant proteins. 41
Figure 2.6. Expression of MBP-KRAS^{WT} human recombinant protein. 43
Figure 2.7. Human recombinant MBP-RAS expresses and is stable..... 45
Figure 2.8. Co-immunoprecipitation results investigating putative KRAS/NRAS heterodimers 47
Figure 2.9. Co-immunoprecipitation results to detect KRAS homodimers. 48
Figure 2.10. Reduced NRAS expression decreases proliferation in mutant KRAS lung adenocarcinoma cells..... 50
Figure 3.1. Proteomic profiling identifies global differences in RIT1 and KRAS mutants as determined by LC-MS/MS can be validated by Western blot. 57
Figure 3.2. Gene set overlap analysis identifies epithelial-to-mesenchymal genes as a key signaling pathway in RIT1 and KRAS mutants. 59
Figure 3.3. RIT1^{M90I} drives an epithelial-to-mesenchymal transition similar to KRAS mutants. 61
Figure 3.4. HLA proteins are down-regulated by RITM90I and KRAS mutants. 63
Figure 3.5. Class I MHC complex proteins correlate with HLA protein expression. 65
Figure 3.6. Understanding loss of class I MHC complex 67

Figure 3.7. LFC of EGFR phosphorylation sites in RIT1-mutant versus KRAS-mutant cells. 69

DEDICATION

Dedicated to my grandpa who passed away from cancer before I was able to meet him. I also dedicate this to my best friend Olivia who was diagnosed with cancer a couple years ago. She continues to inspire me with her grace and bless me with her friendship.

Chapter 1. INTRODUCTION

Somatic mutations in the RAS family genes (K-,N- and H-RAS) are found in ~ 30% of all tumors[1]. Specifically, *KRAS* is mutated in ~30% of lung adenocarcinomas and over 90% of pancreatic cancer[2-5]. Over 60,000 lung cancer patients in the United States are annually diagnosed that are harboring *KRAS*-mutations. While small molecule inhibitors have been developed to target 'driver' mutations in *EGFR* and *ALK*, patients with *KRAS*-driving mutations are primarily treated with chemotherapy[2,6], or with PD-1/PD-L1 immunotherapy[7], although inhibitors to the $KRAS^{G12C}$ variant are now in clinical development[8,9]. This underscores the importance of continuing to understand RAS biology in order to develop targeted therapeutics for treating mutant KRAS-driven cancers.

1.1 RAS PROTEINS

RAS proteins are a ubiquitously expressed family of small GTPases (Figure 1.1). GTPases hydrolyze GTP and function as molecular switches to govern a wide variety of cellular processes[10]. GTPase signaling activity is regulated by binding to GTP or GDP, because the active GTP-bound state results in a conformational change. There are 3 genes encoding 4 proteins that constitute the canonical RAS family: KRAS4A, KRAS4B, NRAS, HRAS[11]. KRAS has two isoforms KRAS4A and KRAS4B, which differ in exon 4. RAS proteins contain a catalytic region known as the G-domain, two switch domains, and a hyper variable region. There is ~80% homology between the RAS family proteins in the G-domain, residues 1-166[11]. While the G-domain is highly conserved in amino acid sequence, codon usage is different. KRAS uses more rare codons compared to HRAS; HRAS uses less rare codons[12,13].

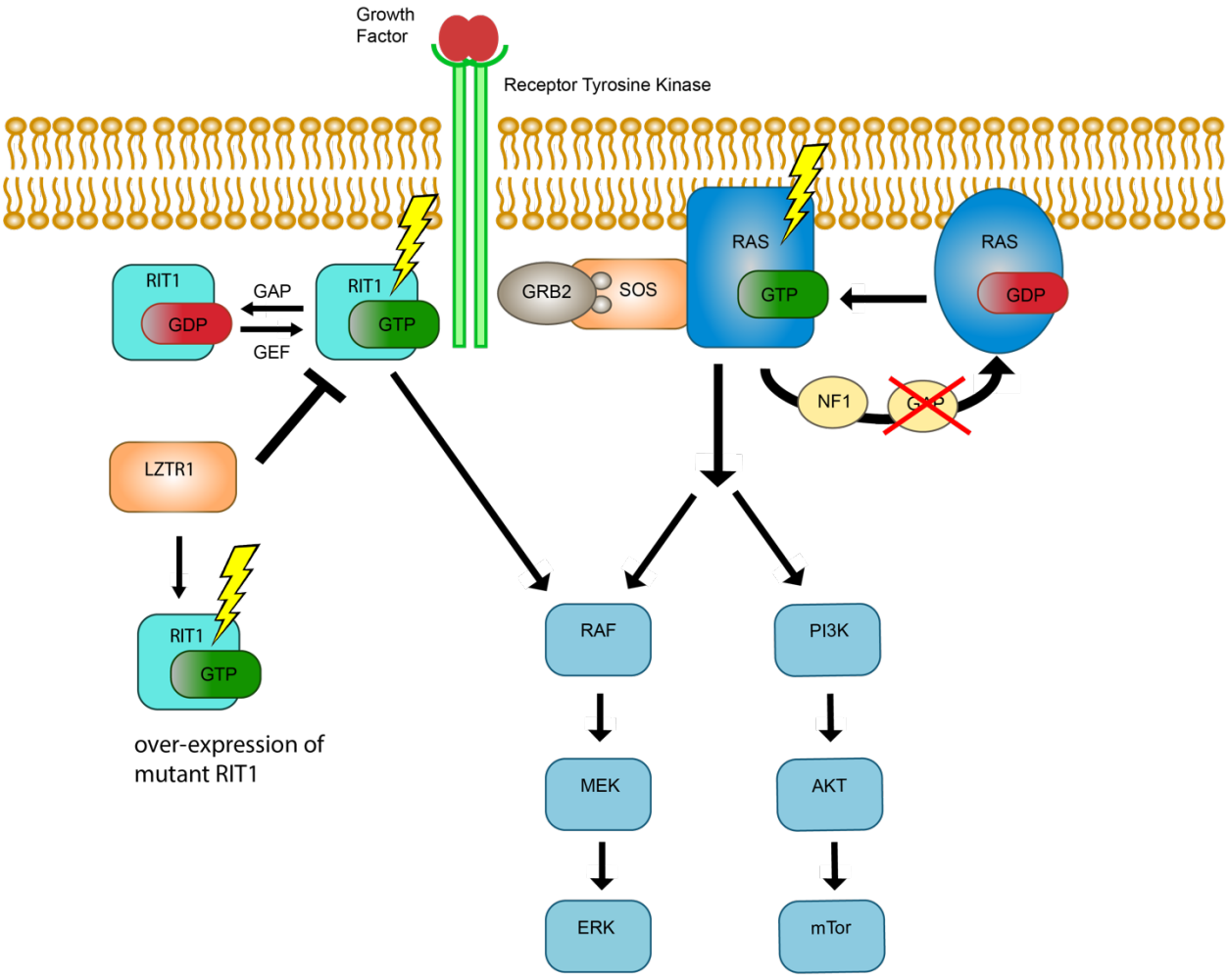

Figure 1.1. Schematic of oncogenic RAS and RIT1 constitutively active signaling.

RAS and RIT1 are GTPases. Oncogenic somatic mutations of RIT1 and RAS drive tumorigenesis through constitutively active signaling to important downstream effectors such as RAF family of proteins and PI3 kinase. Mutant RIT1 inhibits the interaction with LZTR1, and escapes degradation mediated by LZTR1.

This use of rare codons has shown to reduced translation efficiency of KRAS[12,13]. It is postulated that mutant KRAS expression levels can drive tumor formation, but are low enough to evade senescence; conversely, mutant HRAS protein expression levels may be too high to be tolerated, leading to senescence or apoptosis[13,14].

While there is functional overlap between the RAS family members, they are not fully reduntant[15]. *In vivo* embryonic knockouts of RAS family members determined that Kras knockout, but not Nras or Hras knockout, is embryonic lethal. Murine models deficient for Kras expression (*Kras*$^{-/-}$) died around day E12 and none survived to birth[15]. In this study, Kras$^{-/-}$ embryos contained defects in the fetal liver microenvironment resulting in a smaller liver size. In order to understand the functional overlap between Kras and Nras, Johnson *et al* generated Nras$^{-/-}$;Kras$^{+/-}$ murine models. Interestingly, almost 70% of embryos died between E10 and E12, and the remainder died perinatally. Therefore, Kras wildtype expression is required for the survival of Nras deficient mice.

The extensive homology between K-, H-, and NRAS does not extend into the hyper-variable region (HVR). The hyper-variable region is the C-terminal 19-20 amino acids residues of RAS proteins and contains the CAAX domain[11]. After translation, RAS proteins undergo multiple posttranslational modifications. The initial step removes the 3 final amino acids of the CAAX motif to produce an intermediate form of the RAS protein that contains C186 at the C-terminus[16]. This is commonly called Step 1 of RAS processing[17]. The CAAX domain is modified by polyisoprenylation and is required for this Step 1 processing[17,18]. The intermediate form of the RAS protein has increased hydrophobicity but is still primarily found in the cytosol. Polyisoprenylation is added post-translationally to RAS proteins on residue C186 residue in the CAAX domain and is required for RAS proteins to associate with the plasma membrane[17]. RAS proteins are unable to localize to the plasma membrane if residue C186 is mutated, and

nonisoprenylated RAS proteins localize to the cytoplasm[18]. Nonisoprenylated RAS proteins do not transform NIH3T3 cells due to the cytosol localization, not a result of biochemical changes[18]. During this processing, the intermediate and the mature RAS proteins become methylated; no methylation was detected in the initial form of the RAS translation product[16].

Additionally, some RAS proteins receive a palmitoyl post-translational modification during processing. Hancock *et al* observed that palmitoylation is not necessary for transformation. Palmitoylation of HRAS (originally called p21HRAS) occurs at residues C181 and C184; however, KRAS4B (originally called p21KRAS4B) is not palmitoylated[17]. While palmitoylation is not necessary for membrane association, it does increase the affinity of the interaction[17,18]. KRAS4B does not contain a cysteine residue upstream of C186. Instead, KRAS4B contains a polybasic stretch in its hypervariable region, which increases the positive charge of the region[17]. The polybasic stretch strengthens the anchorage of KRAS4B to the plasma membrane by increasing the electrostatic interactions with the phospholipid groups in the membrane.

The observations that signaling occurs when RAS proteins are localized to cell membranes led to the development of farnesyl transferase inhibitors (FTIs) as potential therapeutics to impede mutant RAS tumorigenesis. However, FTIs are unsuitable as potential therapeutics for KRAS and NRAS mutant cancer, because KRAS and NRAS become geranylgeranylated when treated with FTI[19]. Geranylgeranylated KRAS and NRAS remain bound to the plasma membrane where they are able to signal to downstream effector proteins. A key study describing this interesting observation concluded that RAS proteins in the DLD-1 colon cancer cell line become geranylgeranylated when cells were treated with SCH56582, a farnesyl transferase inhibitor[19]. DLD-1 cells have a mutant KRAS allele. This study was extended by transfecting COS cells with individual RAS vectors, followed by SCH56582 treatment in order to determine if HRAS and

NRAS may be geranylgeranylated similar to KRAS. HRAS, unlike KRAS and NRAS, is not able to be geranylgeranylated upon FTI treatment. Therefore, HRAS remains unprenylated, and in the cytosol. This highlights how the biological differences between proteins in the RAS family can dictate the efficacy of potential therapeutics.

In addition to localizing to the plasma membrane, KRAS and NRAS can localize to the mitochondrial membrane[20]. Recent work has determined that KRAS4A additionally localizes to the outer mitochondrial membrane and interacts with HK1, exerting metabolic changes in glucose consumption[21]. Previous literature has primarily focused on the canonical signaling of RAS proteins at the plasma membrane; however, future work may continue to discover the unknown about RAS signaling at the mitochondrial membrane.

1.2 RAS REGULATION

1.2.1 *RTK/Ras Activation*

RAS proteins are active and bind to effector proteins when bound to GTP and inactive when bound to GDP (Figure 1.1). RAS proteins have a very high affinity for GTP. As small GTPases, RAS proteins possess the innate ability to hydrolyze GTP. However, RAS proteins rely on GTPase activating proteins (GAPs) to make the hydrolysis process efficient leading to GDP-bound inactive RAS[22]. Conversely, Guanine exchange factors (GEFs) induce a conformational change in RAS proteins; this conformational change allows for the release of GDP and the binding of GTP leading to active RAS.

There are several RAS GEFs that are regulated by different mechanisms. Growth factors stimulate RAS through the RAS GEF Son-of-Sevenless (SOS). RAS in the plasma membrane is activated when SOS translocates from the cytoplasm to the plasma membrane[23]. The translocation is mediated by GRB2, an adaptor protein, which contains a SH3-SH2-SH3-domain. The SH3

domains bind to the proline-rich region of SOS, and with its SH2 domain to the phosphorylated tyrosine kinase receptors. SOS is recruited to the plasma membrane where RAS is located. SOS contains a CDC25-homology domain specific for RAS and a C-terminal proline-rich region. CDC25 is the RasGEF in *Saccharomyces cerevisiae*[24]. Translocation is controlled by negative feedback loop as a result of ERK phosphorylation of SOS, resulting in its dissociation from GRB2[25].

1.2.2 *Ras effectors*

There have been many RAS effector proteins that have been reported in cancer: RAF, PI3K, RalGDS, Ras effector 1A (NORE1A), Af6, phospholipidase C (PLC), Ras and Rab interaction 1 (RIN1), T cell lymphoma invasion and metastasis-inducing protein (TIAM), and growth factor receptor 14 (Grb14) (summarized in Stephen 2014)[26]. RAS effector proteins contain a RAS-binding domain that typically interacts only with a specific conformation of RAS. When RAS proteins are in the activate state, bound to GTP, the RAS-binding domain allows for effector proteins, such as, RAF and PI3K, to physically bind to RAS proteins. The effector domain in the different RAS proteins (K-, N-, and H-RAS) are identical and are capable of binding the same effector proteins[12]. While there are overlapping biological functions, there are distinct biological difference between K- N- and H-RAS[12,15,27]. Today it is not known the reasons underlying the different biological functions in the RAS family, however, some hypotheses have been put forward. For example, subcellular compartmentalization can regulate the accessibility of RAS proteins to their effectors and activators[28]. Another reason for the biological differences observed between RAS isoforms could be due to different protein expression levels[13]. Although RAS isoforms have extensive homology at the amino acid level, the specific codons vary between RAS isoforms. KRAS uses more rare codons than HRAS. The functional effect of this increase in rare

codon utilization causes reduced translation efficiency and a decrease in KRAS protein expression[29]. Furthermore, even different KRAS missense mutations have different binding affinities and altered nucleotide exchange rates[30]. These differences may account for the different prevalence of each protein in cancer and other diseases.

The RAS-RAF interaction leads to the signaling cascade leading to MEK and ERK phosphorylation and increased cellular proliferation[31,30]. Indeed, given the high affinity RAS proteins have for RAF proteins, it is postulated that other effectors and GAPs cannot compete with RAF proteins[30]. The RAS-PI3K interaction signals through AKT and mToR to affect cellular survival[32]. Both of these interactions occur when RAS is bound to GTP, and at the plasma membrane.

Additionally, different effector proteins may reside in different locations within the cell besides at the plasma membrane. KRAS4A allosterically binds to hexokinase1 (HK1) and this interaction requires outer mitochondrial membrane localization, prenylation and for KRAS to be GTP bound[21]. Hexokinase1 (HK1) is a canonical component of glucose metabolism, and localizes to the outer mitochondrial membrane[33]. HK1 interacts preferentially with KRAS4A and NRAS over KRAS4B and HRAS. When KRAS4B and HRAS are artificially targeted to the outer-mitochondrial membrane they can physically interact with HK1. Both mutant KRAS4A and KRAS4B increase glucose consumption in HEK293T cells; however, mutant KRAS4A induces a much greater glucose consumption. Indicating the importance of exon 4, disrupting exon 4 with CRISPR resulted in a decrease in glucose consumption in mutant KRAS lung and pancreatic cancer cells. HK1 is necessary in the mechanism by which KRAS4A stimulates a greater glucose consumption than KRAS4B. This study suggests that the preference of KRAS4A for HK1 is a consequence of its differential trafficking to the mitochondrial outer membrane.

1.2.3 *Constitutively active mutations*

RAS proteins have a "hot spot" of somatic mutations at residues G12, G13 and Q61[34,35] (Figure 1.2). These mutations impair the association with and inactivation of RAS by GAPs generating constitutively active RAS. The Q61 residue is the catalytic site of KRAS and its mutation strongly inhibits the hydrolysis. RAS^{Q61} wildtype adopts a conformation not observed with the mutants; this particular conformation allows for GTP hydrolysis to be catalyzed[36]. Glutamine 61 forms a hydrogen bond with residues Arg789 of GAPp120 to allow the nucleophilic attack of a water molecule. A RAS protein containing a leucine at position 61 (RAS^{Q61L}) cannot activate the nucleophilic water molecule, because of the leucine side chain. There is also a decrease in the intrinsic hydrolysis for mutations in G12 and G13[30]. Modeling indicates that the side chains of other residues at positions 12 and 13 are within van der Waals distance to residue 61; this may limit the ability for Q61 to coordinate the nucleophilic attack[30]. $KRAS^{G12}$ mutants, which substitute glycine for another amino acid, have reduced GTP binding and/or catalysis[36]. There are no major differences in structure between wildtype and mutant G12V, except for the presence of the side-chain at residue 12[37]. This is one of the challenges in designing inhibitors specifically for KRAS mutants that also do not impede the function of wildtype KRAS. The structure of KRAS contains 1 six-stranded β-sheet, 5 α-helices, and 10 connecting loops[37]. Loop L1 is important and adopts a rigid, inflexible conformation because of the interactions between L1 and the β-phosphate. Due to the inflexible nature of loop L1, G12V mutations expose the hydrophobic side-chain of valine to the solvent; this is also why G13 is an important residue.

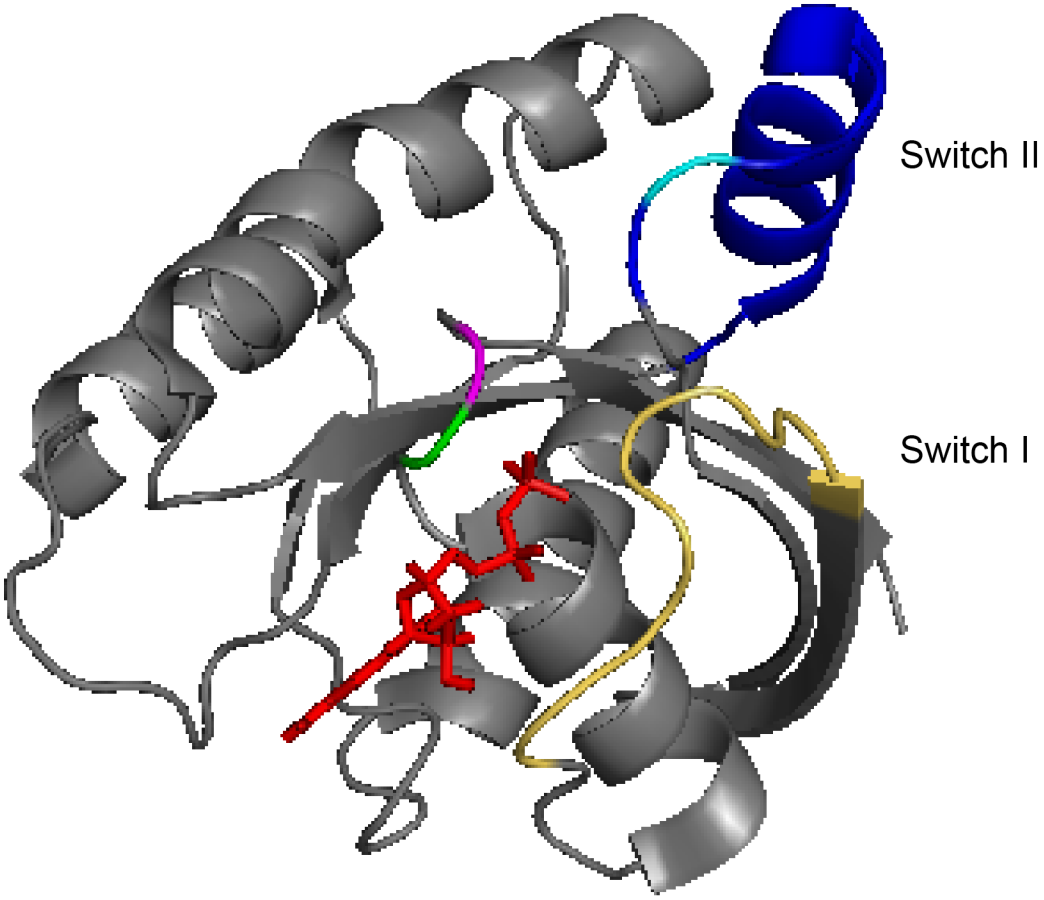

Figure 1.2. Human wildtype KRAS bound to GDP.

The crystal structure of human wildtype KRAS has been resolved. The switch I domain is labeled in yellow. The switch II domain is labeled in blue. Residue G12 is labeled in magenta. Residue G13 is labeled in green. Residue Q61 is labeled in light blue. GDP is depicted in red. (PyMOL; PDB: 4OBE)

1.3 RAS DIMERS

Recently, emerging in the field of RAS biology is the idea that KRAS has the ability to form homodimers. However, RAS homodimers are controversial, and a lot remains unknown.

Previous studies identified nanoclusters containing 5-8 RAS monomers[38-40]. These nanoclusters served as RAS signaling scaffolds to recruit effector proteins such as RAS and PI3K to the plasma membrane. These initial observations were with immuno electron microscopy. Due to the technical limitations of immuno electron microscopy, additional studies were necessary which would allow for increased resolution of the RAS nanoclusters[41]. This study revealed that these 'clusters' were primarily RAS dimers, and higher order oligomers were rare; this result contrasted previous notions that RAS proteins function as monomers, and supports the idea that RAS proteins dimerize[41].

In order to determine if MAPK activation resulted from the formation of RAS dimers, or resulted from RAS overexpression increasing the RAS concentration at the plasma membrane, researchers used an artificial dimerizing agent and KRAS fusion proteins[41]. KRAS was fused to the FKBP-dimerizing domain. Upon treatment with the dimerizing agent, AP20187, KRAS monomers are induced to form artificial dimers without overexpressing KRAS above endogenous levels, and without increasing plasma membrane concentration. Subsequently, the KRAS homodimers were detected using photo-activated light microscopy (PALM), and MAPK activation was measured by ERK phosphorylation. This study concluded that dimerization does not depend upon GTP binding. However, the CAAX domain is required for KRAS homodimer formation. When mCherry was fused to the CAAX domain, mCherry-CAAX aggregated similar to mChery-$KRAS^{WT}$ and mCherry-$KRAS^{G12D}$. Furthermore, when the CAAX domain was mutated to SAAX, the KRAS-SAAX mutant did not localize to the plasma membrane and did not

activate MAPK signaling, even when treated with the dimerizing agent. Therefore, the KRAS-SAAX mutant did not activate downstream MAPK signaling. This study postulated that it is the KRAS homodimers that led to the recruitment and activation of RAF. However, the possibility that the dimers occur using the G-domain could not be excluded. Additionally, it is unknown the role that KRAS homodimers may have on other downstream pathways, like PI3K signaling.

Another study reports two possible conformations of KRAS4B homodimers[42]. This reports that the HVR stabilizes the KRAS oligomeric structure. Increased stability was observed using isothermal calorimetry and fluorescence resonance energy transfer. This finding could possibly support the conclusion in the Nan *et al* study, that the CAAX domain is required for KRAS homodimers as the CAAX domain is contained in the HVR region of RAS proteins. This requirement of the HVR may explain the observation that RAS dimers are better observed in the cellular context because the HVR increases the concentration of RAS proteins at the plasma membrane[4].

It has been postulated that the ability to form dimers is observed across the RAS family of proteins[4,43]. As previously described, KRAS contains 5 alpha helices (Figure 1.2)[37]. The proposed α4- α5 KRAS homodimer would have the binding interface between the α4 helix of one KRAS monomer and the α5 helix of the second KRAS monomer[4]. The α4- α5 KRAS homodimer structure overlaps the interface identified in NRAS molecular modeling. The key residues at this dimer interface are: R135, D154 and R161[4,43]. One study concludes that the dimer interface is distinct from the interface used to bind GAPs and GEFs, while other study postulates that RAS regulatory proteins and effectors compete with β–sheet dimer interface[4,42].

A study conducted by Ambrogio *et al* detected KRAS homodimers in HEK293 cells using fluorescence energy transfer[6]. This study demonstrated the importance of Kras homodimers in

mutant Kras-driven lung cancer *in vivo*. A D154Q mutation, which abrogates the ability for Kras to form homodimers, impeded the tumorigenesis in $Kras^{G12D}$ murine models.

The majority of studies have focused upon RAS protein functions at the plasma membrane, as a result of post-translational modifications to the CAAX domain[20,44]. As a result of differential post-translational modifications, RAS proteins segregate into distinct nanoclusters[44], therefore rendering the possibility of RAS heterodimers difficult to explain. However, the traditional role of RAS proteins functioning only at the plasma membrane has been challenged by the observations that RAS proteins and binding partners can additionally be found at endomembranes of subcellular components[20,45]. As discussed above, KRAS and NRAS were shown to localize to other locations, one of them being the mitochondrial[20,46,47]. Mouse embryonic fibroblasts deficient for NRAS or KRAS exhibited abnormal mitochondrial morphology and impaired mitochondrial function[20]. Recently, it was postulated that an observed dependence of *KRAS*-mutant cells on mitochondrial translation may result from signaling directly at the mitochondrial membrane[46]. While there has been extensive research into the localization of RAS proteins at the plasma membrane, RAS/RAS heterodimers may occur at specific subcellular components with functional consequences, and this merits further investigation.

It is unknown if KRAS forms heterodimers with different RAS family members, and if this potential RAS/RAS heterodimer presents an opportunity for targeted therapeutics. Abrogating dimers may inhibit tumorigenesis in over 60,000 annually diagnosed lung cancer patients in the United States harboring *KRAS*-mutations.

1.4 RIT1 BIOLOGY

RIT1 (RAS-like in all tissues) is a small GTPase in the RAS superfamily and contains similar features to the canonical RAS family members[48,49]. RIT1 (originally called Rit) and RIT2

(originally called Rin) define a sub-family branch in the RAS superfamily tree. The RIT1/RIT2 subfamily groups with the RAS, RAL, MRAS and RRAS families; the RIT1/RIT2 subfamily is most divergent from the RAP subfamily[50]. Similar to most RAS proteins, RIT1 is ubiquitously expressed (Figure 1.3). However, RIT2 is expressed only in neuronal tissue. Like other RAS proteins, RIT1 is a small GTPase and is active when bound to GTP[48,49]. Initial studies, utilizing His-tagged fusion proteins in a nucleotide binding assay demonstrated the ability of RIT1 and RIN to bind to GTP and GDP.

RIT1 functions as a small GTPase, which is similar to other members of the RAS superfamily. A biochemical study by Shao *et al* utilized recombinant proteins to establish RIT1 as a GTPase[49]. This study by Shao also demonstrated that RIT1 releases non-hydrolyzable GTP at a faster rate than GDP. This result was interesting because RAS proteins have a high affinity for GTP and rely upon GAPs and GEFs in order to regulate the amount of time RAS bound to GTP or GDP. After GEFs stimulate the release of GTP or GDP, RAS proteins predominately rebind to GTP, due to the high concentration of GTP in the cell. However, due to the high rate of GTP dissociation, GAPs and GEFs likely have a limited role in regulating RIT1 activity. While GAPs and GEFs regulate RAS activity, it has been additionally demonstrated that intrinsic rates of hydrolysis have important biological effects[30]. RIT1 has a faster intrinsic rate of GTP dissociation relative to most RAS proteins in the superfamily. When compared to RIT1, at same conditions, less than 10% of non-hydrolyzable GTP was dissociated from recombinant HRAS. Residue Gly79 in RIT1 is analogous to Q61 in RAS[(51)]. This study revealed that Gly79 is important to the intrinsic GTPase activity of RIT1. $RIT1^{Q79L}$ mutant exhibited a reduced rate of GTP hydrolysis and a 3.5-fold increase in the rate of GDP dissociation relative to wildtype Rit.

RIT1 and RIT2 are 65% homologous, with the most extensive homology (74%) in the central 167 residues[48]. RIT1 has 3 isoforms, and isoform 2 is the most studied; RIT1 contains an extended N-terminal region relative to RAS proteins[51]. RIT1 is found at the plasma membrane and cytosol. RIT2 has an unusual feature, not shared with RAS family or RIT1: it has a C-terminal sequence that binds calmodulin[48]. The significance of this sequence is unclear. Unlike canonical RAS family members, RIT1 does not contain a CAAX domain in its C-terminal region. Although RIT1 does not undergo prenylation or palmitoylation, it does have a polybasic stretch in its C-terminal region of residues 180-194[48,50]. It was demonstrated that this polybasic stretch is required for RIT1 localization to the plasma membrane. RIT1 contains a conserved G2 domain and effector region that are distinct from the RAS family[48,49]. The G2 domain is 100% conserved from human to murine, with an identical sequence. The effector G2 domain is similar to NRAS with 7 of the 9 residues conserved. The similar effector region to the RAS family suggests RIT1 may use similar effectors. Yet the distinctions raise the possibility that there are unique effectors for RIT1 distinct from the RAS effectors. Below I will describe a few studies about RIT1 effector proteins that are known so far.

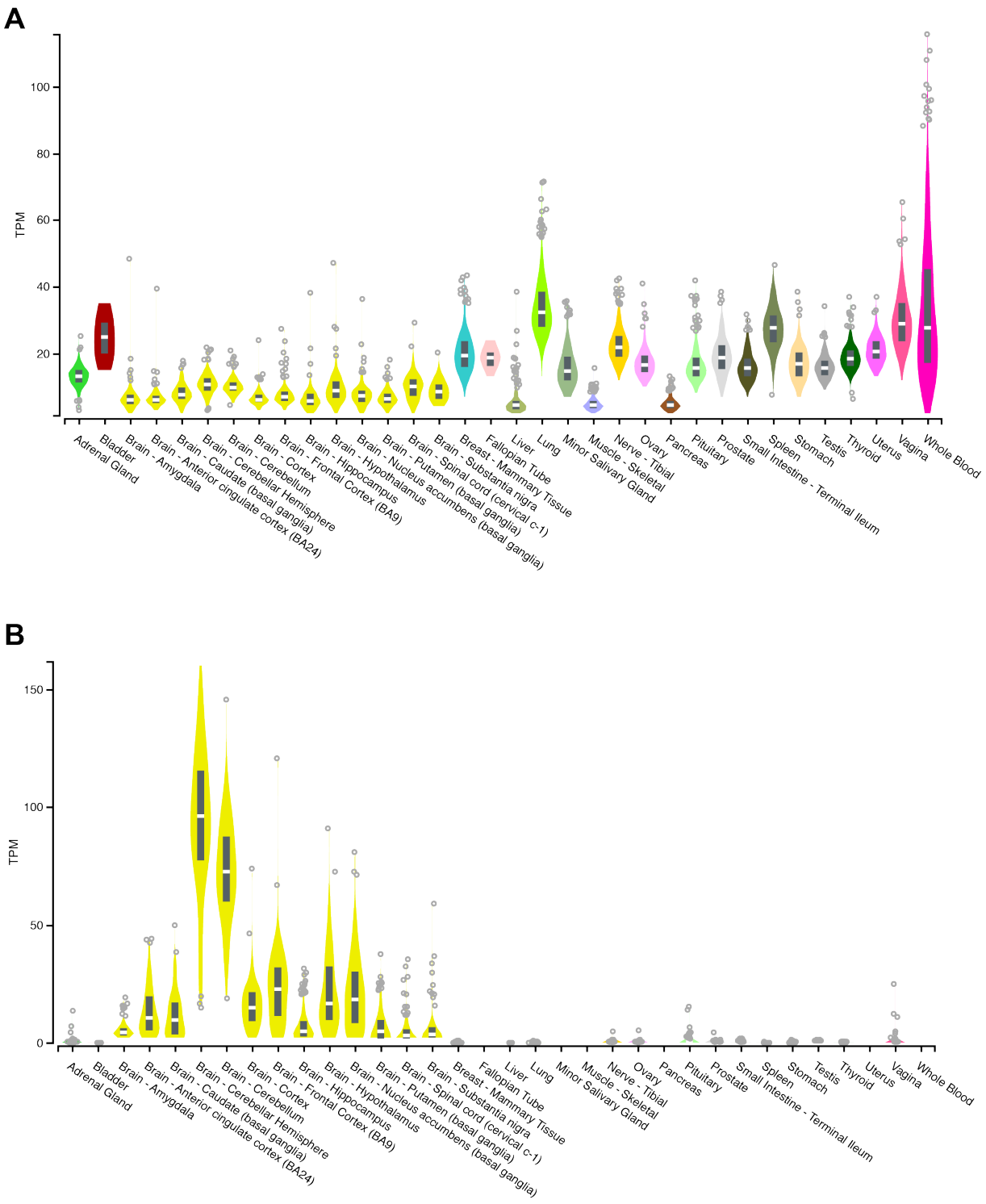

Figure 1.3. Gene expression of RIT1 and RIT2.

A) Tissue-specific gene expression levels of RIT1. RIT1 is ubiquitously expressed. B) Tissue-specific gene expression levels of RIT2 reveal that RIT2 is expressed primarily in neuronal tissues. (GTEx Portal – gtexportal.org)

Since RIT1 and RAS have extensive homology, especially in the effector domain, an early study by Shao *et al* investigated known RAS effectors to search for potential RIT1 effector proteins[49]. This study utilized a yeast two hybrid binding assay to identify RAS effector proteins as RIT1-binding proteins. In this study, a transcriptional activation domain was fused to cDNA of the following known RAS effectors: RAF-RBD, A-RAF, B-RAF, C-RAF, RalGDS-RID, RLF-RID, AF6, RIN1, PI3K p110 (RID = RAS interacting domain; RBD = RAS binding domain). As expected, HRAS bound to all of the investigated proteins, but RIT1 only bound some RAS effector proteins, namely: RalGDS-RID, RLF-RID, AF6[49]. RitS35N, an analogous effector mutant to the RAS^{S17N} dominant negative mutant, did not interact with any of the investigated effector proteins. These results indicate that RalGDS, RLF and AF6 prefer to interact with GTP-bound RIT1 over GDP-bound RIT1. The RIT1-Ral-GDS interaction was confirmed to be GTP-dependent, but additional studies are needed to determine the functional effects of this interaction. It was also observed that RIT1 only interacted with RLF-RID when loaded with non-hydrolyzable GTP, and that HRAS has a higher binding affinity for RLF-RID than RIT1. $RIT1^{Q79L}$ interacted with the known RAS effector proteins in similar fashion to wildtype RIT1. However, this study determined RAF protein kinases were not effectors of RIT1, because no interaction was detected between RIT1 and B-RAF or C-RAF. This result was disproved in later studies confirmed that RIT1 does indeed interact with C-RAF and B-RAF in human cells[52,51], and that RIT1 signals through the MAPK/ERK pathway[50]. Since later studies demonstrated that RIT1 interacts with C-RAF and B-RAF, the negative two-hybrid result may have been an artifact of the study, or there are additional factors required to support this interaction. However, it is interesting that RIT1 is capable of binding to B-/C-RAF but this interaction leads only to B-RAF activation. RIT1 is capable of

activating ERK following receptor tyrosine kinase stimulation, but this varies by cell type and the type of tyrosine receptor activation.

Another study concluded that PAR6 is an effector protein of RIT1[53]. RIT1 binds directly to PAR6 in a RIT1-PAR6-Rac/Cdc42 ternary complex. The RIT1-PAR6 interaction was determined to be GTP-dependent, and that RIT1 binds to the PDZ domain in PAR6. This interaction was determined by co-immunoprecipitation in COS-7 cells with N-terminal Myc-tagged RIT1 and GST-tagged PAR6. The RIT1-PAR6 interaction is specific to the RIT1/ RIT2 subfamily as co-immunoprecipitation with full length Myc-tagged HRAS did not replicate the interaction. A $RIT1^{Y58C}$ mutant was created to model the RAS Y40C mutant that is unable to bind to effector proteins. As expected, the $RIT1^{Y58C}$ mutant did not bind to PAR6. Therefore, indicating that RIT1 binds through its effector domain to the PDZ domain of PAR6 in a GTP-dependent manner. The functional role of RIT1-PAR6-Rac/Cdc42 complex was determined using a foci formation assay in NIH3T3 cells. It was concluded that the RIT1-PAR6-Rac/Cdc42 complex was necessary for foci formation. However, the RIT1-PAR6 interaction is controversial and may be more complex than initially determined and further studies are needed[50].

Additionally, RIT1 signals to p38 MAPK. RIT1 activates p38 in response to diverse stimuli including reactive oxygen species (ROS) to regulate cell survival[50]. It has been demonstrated that ROS-mediated p38 activation is impeded in *Rit1* knockout MEFs. RIT1-p38 activation lead to MK2 activation with HSP27. HSP27 is a scaffolding protein[50], and MK2 is a kinase essential for tumor necrosis factor synthesis[54]. It was demonstrated that HSP27-MK2-p38 complex is required for RIT1-dependent AKT activation. Furthermore, stress dependent ROS-p38 activated- AKT scaffold activation regulated cell survival. RIT1 co-immunoprecipitated with p38, AKT, MK2, and HSP27. However, HRAS did not immunoprecipitate with those proteins. Silencing RIT1 or

inhibiting p38 or MK1/2 leads to CREB-dependent transcription, inducing expression of Bcl-2 and Bcl_{XL} anti-apoptotic proteins, to promote cell survival.

While some additional effector proteins for RIT1 have been identified, the full spectrum of RIT1 effector proteins remain to be elucidated.

1.5 "RAS"-OPATHY – NOONAN SYNDROME

Mutations in the RAS/MAPK pathway cause Noonan Syndrome, a congenital disorder characterized by cardiac defects, facial dimorphism and short stature. Germline mutations in *KRAS, NRAS*, *PTPN11*, *SOS1*, *BRAF*, *RAF1 (CRAF)*, *MAP2K1* and *MAP2K2* have been identified to cause Noonan Syndrome[55-57]. Noonan syndrome shares some overlapping phenotypic features with Costello syndrome, which is caused by germline mutations in HRAS[56-58]. Additionally, patients with Noonan Syndrome exhibit a predisposition to RAS-driven Juvenile myelomonocytic leukemia; approximately 25% of Juvenile myelomonocytic leukemia patients have germline KRAS and NRAS mutations[56, 55]. A dysregulation of the RAS/MAPK pathway causes Noonan Syndrome.

1.5.1 *RAS germline mutations*

The germline mutations that are found in Noonan Syndrome are functionally different than those found in RAS-driven cancers[56,55]. A couple of representative KRAS variants identified in Noonan Syndrome are: T58I, and V14I. Like the activating mutations in RAS-driven cancers, these mutations reduce intrinsic GTPase activity, thereby activating RAS signaling, but unlike the mutations in cancer, the GTPase activities of Noonan Syndrome can still be activated by neurofibromin and p120 GAP. The $KRAS^{V14I}$ mutation affected the innate GTPase activity less than wildtype but was more functionally responsive to GAP stimulation than G12D, which was

unresponsive[56]. Similarly, the $KRAS^{T58I}$ mutation was less responsive than $KRAS^{WT}$; interestingly, $KRAS^{T58I}$ was specifically more responsive to p120 GAP stimulation than to another GAP, neurofibromin. These mutations render the protein less responsive to GAP-mediated hydrolysis than wildtype KRAS, but they still retain some responsiveness relative to the strong KRAS mutations found in cancer. A couple of representative NRAS mutations found in Noonan Syndrome are at T50I and G60E[55]. G60E is functionally similar to the Q61 mutation which are found in RAS-driven cancers; $NRAS^{G60E}$ mutants are bound to GTP more than GDP and are resistant to GAP activity. Resolving the crystal structure revealed that the NRAS T50I and G60E mutations did not result in a significant change in the protein structure.

These findings have led to the idea that Noonan Syndrome is caused by germline RAS mutations, which weakly reduce the overall GTP hydrolysis rate, compared to oncogenic mutations. However, mutations that render the RAS protein completely resistant to GAP activity are developmentally lethal, and thus occur only as somatic mutations[56,55]. *KRAS* mutations are more associated than NRAS mutations with severe developmental delays and learning issues[59].

1.5.2 *RIT1 germline mutations*

Novel *RIT1* mutations were identified in patients with Noonan Syndrome. Whole exome sequencing identified 9 mutations in *RIT1*, corresponding to ~9% (17/181) of patients previously classified to have an unknown Noonan Syndrome mutation[57]. The following previously known Noonan Syndrome mutations were negative in the 181 patients: *PTPN11*, *KRAS*, *HRAS*, *SOS1*, *BRAF* (exons 6 and 11-16), *RAF1* (exons 7, 14, and 17) *MAP2K1* and *MAP2K2* (exons 2 and 3), and exon1 in *SHOC2*. Noonan syndrome RIT1 mutations occur throughout the protein in the G1, switch I and switch II domains; the location of RIT1 mutation in Noonan Syndrome contrast the location of mutations in HRAS found in Costello Syndrome, which occur at residues G12, and

G13 in the G1 domain[57,58]. Overexpression of mutant RIT1 cDNA results in increased ELK1 transactivation. The following Noonan Syndrome RIT1 mutations were studied: S35T, A57G, E81G, F82L, G95A. $RIT1^{S35}$ corresponds to RAS^{S17}, which when mutated to N is dominant negative[49,51]. However, $RIT1^{S35T}$ cells exhibited the increase in ELK1 transactivation that was not expected for a dominant negative effect, indicating the RIT1 mutations observed in Noonan Syndrome are gain-of-function mutations. Cardiac abnormalities are a feature of Noonan Syndrome[55-57]. In the Aoki *et al* study, the incidence of hypertrophic cardiomyopathy is greater in RIT1-mutant Noonan Syndrome than the overall rate of Noonan Syndrome. 70% of patients with RIT1 mutations had cardiac hypertrophy (12/17) compared to the 20% occurrence in Noonan Syndrome overall (25/181).

Noonan Syndrome has been modeled in model organisms, such as zebrafish and murine models[52,57]. The role of RIT1 in development is conserved. Introducing mutant RIT1 mRNA into zebrafish results in developmental abnormalities, such as: craniofacial abnormalities, hypoplastic chamber, and enhanced yolk sac. Some of these abnormalities are reminiscent of Noonan Syndrome. Approximately 70% of embryos exhibited significantly slower development.

1.5.3 *Treatments*

The challenge in clinically diagnosing Noonan syndrome is that, while it is autosomal dominant, the expression is variable and heterogenous[59]. However, since the Noonan Syndrome phenotype affects individuals from birth, correct post-natal diagnosis is important because Noonan Syndrome treatment requires a multifaceted approach to manage and control[59]. Cardiac abnormalities are a feature of NS, and over 50% of Noonan Syndrome patients have an abnormal electrocardiogram; hypertrophic cardiomyopathy is present in ~20% of Noonan Syndrome cases, and higher incidence for specific mutations, such as RIT1 and RAF1[57,59]. Therefore, adults with

Noonan Syndrome will require follow up cardiac monitoring. Although most patients have mild pulmonary valve stenosis, some patients may have a more severe case that requires intervention such as a balloon valvuloplasty, or, in severe cases, a pulmonary valvectomy or pulmonary homograft during childhood[59]. Noonan Syndrome/myeloproliferative disorder (MPD) is condition found in infants. Noonan Syndrome/MPD is similar to Juvenile myelomonocytic leukemia, but with a better outcome while some infants will develop aggressive Juvenile myelomonocytic leukemia, some will improve by year 1 without clinical intervention[59]. In a study that identified RIT1 mutations in Noonan Syndrome, one patient developed cancer and was put on standard chemotherapy as treatment[57]. Growth hormones have been used to treat Noonan Syndrome and the efficacy of this treatment has been studied. While Noonan Syndrome is characterized by a lymphatic development disorder, there have been heterogenous and inconsistent results as a result of growth hormone treatment[59]. This inconsistency may be a result of the genetic heterogeneity of mutations that underlie Noonan Syndrome and requires additional studies to elucidate the role, and responsiveness of growth hormone treatment in Noonan Syndrome patients. PTPN11 positive patients have been shown to have less response to growth hormones treatment than PTPN11 negative patients[59]. However, since this study had differences in efficacy from short versus long term studies, this result is controversial and may be a feature of the study design. Noonan Syndrome presents many clinical features and requires accurate post-natal identification and a multidisciplinary treatment approach.

1.6 RTK/RAS SIGNALING IN LUNG ADENOCARCINOMA

Somatic mutations in the RAS family (K-,N- and H-RAS) are found in ~ 30% of all tumors[1]. Incidence of mutations vary between KRAS, NRAS, and HRAS. RAS proteins are mutated at different rates in human cancers; for example KRAS mutations are the most prevalent of all RAS

missense mutations (84%), followed by NRAS (~12%), and HRAS (~4%)[60]. Not all RAS mutations are the same. Mutations affect the intrinsic hydrolysis of KRAS, which is thought to have a biochemical functional effect, irrespective of the interaction with GAPs and GEFs[30].

Different RAS genes are mutated in different types of cancers. Within certain cancer types a particular RAS gene may be mutated more frequently than another RAS gene. There are differences in the incidence of KRAS mutations depending upon cancer tissue type[61]. For example, *KRAS* is mutated more frequently in lung adenocarcinoma (LUAD), than HRAS[2]. KRAS is almost the exclusive driver of pancreatic ductal adenocarcinoma, accounting for over 95% of driving mutations[5]. Furthermore, a particular RAS mutation may be more prevalent in a certain type of cancer depending upon the tissue type. For example, G12C very common in lung cancer, but rare in PDAC. It has been suggested that this may be due to selection for a particular mutation when tumorigenesis originated[62]. This selection may be informed by pressures to select the particular RAS protein and mutation that renders the optimal expression level for tumorigenesis.

1.6.1 *KRAS-driven Lung Adenocarcinoma*

KRAS is mutated in ~30% of lung adenocarcinomas and over 90% of pancreatic cancer[2-5]. Interestingly, wildtype KRAS is thought to impede the tumorigenesis driven by its mutant counterpart[3]. In support of this idea, wildtype *KRAS* is lost in patient samples harboring *KRAS* mutations[63], showing that there is a selection against wildtype KRAS function in mutant KRAS lung tumorigenesis. This genetic interaction between wildtype and mutant KRAS could be explained by a recently discovered phenomenon: RAS dimerization. Emerging in the field of RAS biology is the revelation that KRAS can dimerize and KRAS-GTP homodimers activate MAPK signaling[41]. Surprisingly, mutant KRAS dimers are required for *KRAS*-mutant lung tumorigenesis[6]. Ambrogio *et al* identified a specific amino acid, D154, involved in a RAS

dimerization; a D154Q variant of KRAS is unable to dimerize[6]. Interestingly, when the $Kras^{D15Q}$ mutant was introduced to $Kras^{G12D}$ mice, there was a decrease in lung tumors, proliferation, ERK phosphorylation in $Kras^{G12D/D154Q}$ mice models. It is postulated that homodimers may explain the phenomenon of wildtype KRAS attenuating *KRAS*-mutant lung cancer progression and raises the exciting possibility of blocking KRAS dimer formation for therapeutic benefit[6,41].

Additionally, it has been demonstrated that expression of wildtype NRAS and HRAS have a functional role in KRAS-driven cancer[1,64]. Murine models of Nras null mice were chemically treated with urethane, which commonly causes mutation of Kras, to induce lung tumors mutations[64]. The $Nras^{KO/KO}$ mice with Kras mutations exhibited more lung tumors than wildtype Nras mice. There was a very modest increase in the incidence of Kras-induced tumors, in the $Hras^{KO/KO}$ and $Hras^{WT/KO}$ mutant mice compared to mice with wildtype Hras. Conversely, however, in KRAS-driven colon cancer cells, loss of wildtype NRAS had the opposite effect, with a decrease in proliferation, and increased sensitivity to chemotherapy[1]. In this colon cancer study, NRAS and HRAS were knocked down using shRNA. It was found that decreased expression of NRAS, and HRAS, in KRAS-mutant cells caused a decrease in proliferation, as a result of a delayed mitotic cycle. Additionally, a hyper-phosphorylation of ERK and PI3K/Akt signaling pathways. The hyper-activation led to phosphorylation of Chk1 at an inhibitory site, residue S280. More work will need to elucidate the mechanisms behind the contradicting role of wildtype RAS family members in KRAS-driven cancer, as there may be tissue specific effects.

1.6.2 *RIT1-driven Lung Adenocarcinoma*

The TCGA study identified potentially oncogenic mutations in RIT1 in tumors that lacked known oncogenes[2]. RIT1 mutations account for approximately 2% of lung adenocarcinoma cases and are mutually exclusive with other mutations in the receptor tyrosine kinase/RAS/MAPK signaling

pathway. A hot-spot of mutations occurs at residue M90; the change is a methionine to an isoleucine[2,65]. RIT1 mutations typically occur in regions of the protein different from oncogenic mutations in RAS family proteins; not at residues G12, G13, or Q61 which dominate RAS mutations[52]. Nevertheless, RIT1 mutations have the ability to transform cells to harbor a cancer phenotype[52,65]. Soft agar assay in NIH3T3 cells transfected with RIT1 mutations identified in the TCGA study indicated that RIT1-mutant cells exhibit anchorage independent growth[65].

RIT1 oncogenic mutations cluster in the switch II domain, the effector region[50,51,65]. The mechanism by which they activate RIT1 is unclear. One study suggested that the oncogenic mutations inhibit RIT1 degradation, thereby increasing RIT1 levels in the cell[52]. In this study, MEFs expressing $RIT1^{M90I/+}$ had higher levels of RIT1 protein but no change in mRNA expression levels. Additionally, mass spectrometry identified multiple proteins, including LZTR1, as a potential adapter protein for RIT1. The interaction of RIT1 and LZTR1 was confirmed with immunoprecipitation in HEK293T cells. RIT1-GDP bound preferentially to LZTR1 over RIT1 loaded with non-hydrolyzable GTP. Surprisingly, RIT1 mutants did not bind to LZTR1; an exception to this observation is mutant $RIT1^{Q79L}$, which still exhibited decreased binding relative to wild-type RIT1. Over-expressing LZTR1 in HEK293T cells resulted in a decrease of RIT1 protein that could be rescued by bortezomib (proteasome inhibitor); this rescue was not observed with bafilomycin (lysosome inhibitor) treatment. MEFs deficient for LZTR1 had an increase in RIT1 protein stability. Overall, these results suggest that activating mutations in RIT1 increase the abundance of RIT1 and dysregulate MAPK signaling in response to growth factor stimulation.

In the Berger lab a small molecule screen of previously approved inhibitors was assayed for cell viability in a model of RIT1-driven drug resistance[66]. The screen selected for the inhibitors that can block $RIT1^{M90I}$-driven cell survival and cause cell death. The top candidates identified

were alisertib and barasertib, inhibitors of Aurora kinase A and B, respectively. The screen was confirmed by a colony formation assay in NIH3T3 cells; there was a decrease of colonies when $RIT1^{M90I}$ mutants were treated with alisertib. The observed effects of the Aurora kinase inhibitors are specific to RIT1-mutant cells as $KRAS^{G12D}$ cells were unaffected by the inhibitor treatment. Aurora kinase A is upstream of cyclin-dependent kinase 1(CDK1), a critical regulator of the cell cycle[67]. Ectopic expression of active Aurora kinase A overrides the G2 block induced DNA damage. This signaling reactivates CDK1 and occurs through a Chk1-dependent mechanism. Interestingly, Grabocka *et al* proposed a model that the mechanism whereby the knockdown of NRAS or HRAS expression in KRAS-mutant cells decreases proliferation involves Chk1 phosphorylation and DNA damage[1]. SiRNA knockdown of NRAS or HRAS expression in KRAS-mutant cells disrupts G2 DNA damage response by reducing Chk1 activity. Chk1 activity is impaired by inducing phosphorylation of Chk1 at an inhibitory site, residue S280. Loss of Chk1/ATR DNA damage response signaling can sensitize KRAS-mutant cells to previously ineffective DNA-damaging chemotherapies. Therefore, it could be possible that Aurora kinase inhibitors used in the screen would be effective on KRAS-mutant cells if co-treated with Chk1 inhibitors.

1.6.3 *Treatment of RAS- and RIT1-driven Lung Adenocarcinoma*

Certain lung adenocarcinoma tumors have benefitted from targeted therapies such as kinase inhibitors. Small molecule inhibitors have been developed for the tyrosine kinase receptor EGFR[68,69]. EGFR is upstream of RAS proteins and therefore these therapies are ineffective for patients with RAS mutations. However, patients with *KRAS*-driving mutations are primarily treated with chemotherapy[2,6], or with PD-1/PD-L1 immunotherapy[7]. KRAS mutations in cancer have thus far been an elusive and challenging target for targeted therapies[12].

There are many challenges to directly targeting RAS proteins, due to the structure of RAS proteins. RAS proteins do not contain deep pockets where an inhibitor could bind[12]. Additionally, wildtype and mutant RAS proteins have similar structure[37]. Another challenge for the development of RAS-specific therapeutics, is that the inhibitor must be able to distinguish between the RAS proteins, as inhibitors which inhibit K-,N-, and HRAS would probably be too toxic[12]. Furthermore, targeting both KRAS splice variants, KRAS4a and KRAS4b, but not NRAS or HRAS is another challenge.

Future therapies may benefit from targeting a specific RAS mutation. Recently, an inhibitor specifically for $KRAS^{G12C}$ mutations has been developed and has entered clinical trials[8,9]. This inhibitor is specific for G12C mutations as it relies on this residue to create a covalent bond using the cysteine residue in the G12C[8]. These inhibitors allosterically bind the GDP state preferentially and blocks the GDP to GTP exchange. There are currently no prospective therapeutics which target $KRAS^{G12V}$ or $KRAS^{G12D}$ mutations[12].

An alternative to directly targeting RAS proteins is to target the RAS effector proteins. RAF inhibitors were thought to be a possible strategy for KRAS mutant cancers. ATP-competitive RAF inhibitors, such as vemurafenib, were developed to specifically target $BRAF^{V600E}$ mutations. Vemurafenib was selective for the mutant and preferentially bound the oncoprotein over the wildtype BRAF protein, giving hope it would be therapeutically useful[70]. However, ATP-competitive RAF inhibitors paradoxically activate the downstream MAPK signaling in wildtype BRAF cells, a phenomenon known as the RAF inhibitor paradox [71-73]. Drug treatment with ATP-competitive RAF inhibitors induced association of RAF with RAS-GTP and RAF dimerization. Wildtype RAF proteins are typically found in an auto-inhibited state. Below the concentrations necessary to saturate the inhibitor, the RAF inhibitors relieve stimulate downstream MEK

signaling by mitigating auto-phosphorylation of wildtype RAF, when RAS is active. This activation of MEK signaling induces proliferation of mutant RAS cells *in vivo.* However, at saturating concentrations, the inhibitor blocks BRAF downstream MEK signaling[70-73]. Thus, Vemurafenib cannot be used on BRAF wildtype cancers, such as cancers with activated RAS.

It is necessary to continue to understand RAS biology in order to develop improved therapies which target mutant KRAS-driven cancers.

Chapter 2. NRAS IN KRAS-DRIVEN LUNG ADENOCARCINOMA

2.1 INTRODUCTION

In recent years there has been emerging evidence that RAS proteins form homodimers. These homodimers may be required for mutant KRAS-driven tumorigenesis. It is postulated that KRAS homodimers may be transient and weak. Previous studies have relied on fluorescence based assays, or utilized recombinant proteins in order to interrogate RAS homodimers[6,41]. However, it is unknown if RAS proteins can form heterodimers with other RAS proteins.

As previously stated, KRAS homodimers require the CAAX domain to activate MAPK. Wildtype but not SAAX mutant KRAS chimeras containing an artificial dimerization domain could be dimerized upon treatment with the dimerizing agent, AP20187[41]. However, SAAX mutants did not localize to the plasma membrane and MAPK was not activated. Photoactivated light microscopy demonstrated that the hypervariable region (HVR) stabilizes KRAS oligomers[42]. The HVR enhances the concentration of KRAS monomers at the plasma membrane increasing the likelihood of homodimers. KRAS homodimers activate MAPK signaling, as measured by ERK phosphorylation[41]. It's been demonstrated that KRAS homodimers do not depend on GTP or GDP. The ability to form homodimers is a shared property of KRAS-GDP and KRAS-GTP[41,42].

An antibody, NS1, has been created which can selectively bind to HRAS and KRAS but not NRAS[4]. The NS1 antibody does not block SOS mediated exchange, and it disrupts RAS homodimers and downstream RAF activation. As the G-domain is conserved in RAS proteins, it is speculated that the dimer conformation is conserved across Ras family members. The α4- α5 dimer interface is present in $KRAS^{G12D}$ structure (PDB: 4EPR). This interface overlaps residues identified by NRAS dimer molecular modeling. Important residues at the interface of the NRAS homodimer are R135, D154, and R161[43]. Residue D154 has been demonstrated to be a critical

residue in KRAS homodimers, forming an electrostatic bond with R161 on corresponding KRAS molecule[6]. Similarly, residue R161 is proposed as an important residue in NRAS dimerization because of electrostatic interactions[43]. This strengthens the possibility for KRAS and NRAS to form heterodimers, with effects on RAS signaling. The dimer interface described is distinct from that used to bind GAPs and GEFs.

Ambrogio *et al*, utilized fluorescence resonance energy transfer (FRET) to detect KRAS homodimers[6]. When CFP-KRAS and YFP-KRAS bind there is an increase in relative CFP fluorescence signal if the two KRAS monomers are in proximity. This output was used to validate $KRAS^{WT}$-$KRAS^{WT}$ homodimers and $KRAS^{G12V}$-$KRAS^{G12V}$ human cells. Furthermore, these $KRAS^{MUT}$-$KRAS^{MUT}$ homodimers are required for mutant KRAS tumorigenesis. By analyzing the structure of KRAS it was predicted that residue D154 was required for KRAS homodimers. D154 forms a salt bridge with residue R161 on the second RAS monomer. Introducing a D154Q mutation abrogates the ability of $KRAS^{WT}$, and oncogenic $KRAS^{G12V}$, to form homodimers. When the $KRAS^{G12V}$-$KRAS^{G12V}$ homodimers were abrogated *in vivo*, there was a significant reduction in tumor progression as evident by a reduction in tumor volume. Additionally, there was a decrease in proliferation, measured by Ki67 staining, and MAPK activation, measured by ERK phosphorylation.

It has been observed for many years that wildtype KRAS impedes the tumorigenesis driven by its mutant counterpart[3]. Indeed, wildtype *KRAS* is lost in patient samples harboring *KRAS* mutations[63]. It is postulated that homodimers may explain the phenomenon of wildtype KRAS attenuating *KRAS*-mutant lung cancer progression and raises the exciting possibility of blocking KRAS dimer formation for therapeutic benefit[6,41].

Two studies investigated the role of NRAS in KRAS-driven lung adenocarcinoma. As discussed above, one study found that there was an increase in tumors found in $KRAS^{G12V}$ mutant mice deficient for NRAS[64]; conversely, another study found an inverse functional relationship for the role of NRAS in mutant KRAS mice[1]. These studies indicate that there is a functional role for NRAS in progression of mutant KRAS-driven cancer. However, additional studies are necessary to elucidate whether wildtype NRAS behaves like wildtype KRAS and has an inhibitory role in mutant KRAS lung adenocarcinoma progression, or the inverse effect.

While there is emerging evidence of RAS dimers, this remains controversial in the field. There are limitations to the current studies of KRAS homodimers. The fluorescence-based assays, fluorescence resonance energy transfer (FRET) and PALM rely on proximity as a read out for KRAS homodimers[6,41]. No direct binding assay has yet been able to detect RAS homodimers, and no crystal structure has yet been resolved for RAS homodimers. Much more remains to be explored and illuminated about RAS dimers, as it is currently unknown if RAS proteins have the ability to form heterodimers.

Given the challenge in targeting KRAS for effective therapeutics, and that much is still unknown about RIT1 biology, proteomic analysis was performed to define the similarities and differences between RIT1- and KRAS-driven signaling in lung adenocarcinoma. Additionally, mass spectrometry was performed in order to investigate RIT1- and KRAS interacting proteins. The Berger lab performed mass spectrometry and proteomic profiling and this preliminary data was used as the foundation of my thesis research project. This goal of this study was to define KRAS and RIT1 signaling pathways and elucidate KRAS interactors for therapeutic opportunities.

Overexpressing mutant KRAS (G12V or Q61H) in AALE cells has the ability to transform the cells from immortalized tracheal epithelial cells to a cancer phenotype; similar to KRAS, over-

expressing RIT1 transforms epithelial cells[65]. It has been previously demonstrated that $RIT1^{M90I}$ and other oncogenic RIT1 mutations can transform NIH3T3 cells *in vitro* and *in vivo*[65]. However, it was unknown if oncogenic RIT1 can transform human immortalized epithelial cells, AALE cells. Therefore, the following constructs were stably overexpressed in immortalized tracheo-bronchial epithelial (AALE) cell background: Renilla (control), Flag-$KRAS^{WT}$, Flag-$KRAS^{G12V}$, Flag-$KRAS^{Q61H}$, Flag-$RIT1^{WT}$, Flag-$RIT1^{M90I}$ (Figure 2.1A). As expected, based upon rodent models, overexpressing $RIT1^{M90I}$ and $KRAS^{G12V}$ in AALE cells induced cellular transformation to enable AALE cells to form soft agar colonies (Figure 2.1B).

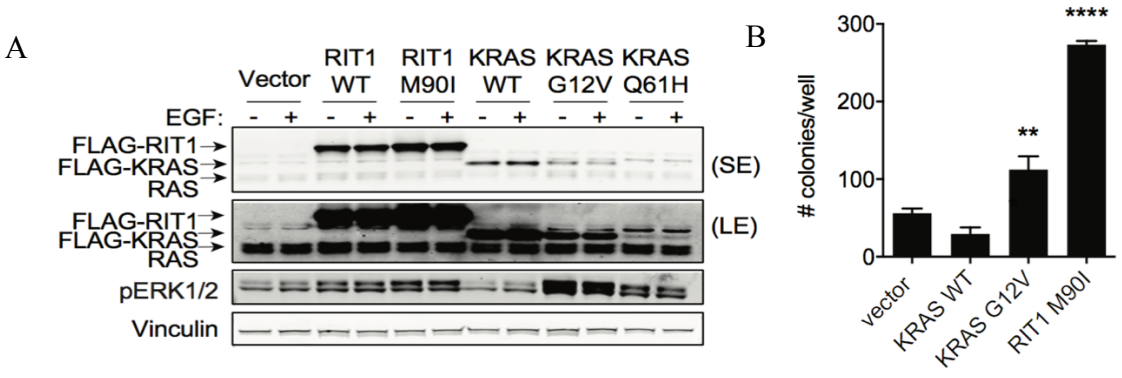

Figure 2.1. Expression of wildtype and mutant RIT1 and KRAS in AALE epithelial cells

Western blot of AALE cell lines over-expressing: Flag-KRAS^{WT}, Flag-KRAS^{G12V}, Flag-KRAS^{Q61H}, Flag-RIT1^{WT}, or Flag-RIT1^{M90I} B. Soft agar colony formation assay of transformed AALE cells. (All data provided by Dr. Alice Berger)

In order to identify the signaling networks modulated by mutant RIT1 and mutant KRAS in lung cancer, each variant was expressed in AALE cells and subjected to global proteome and phosphoproteome profiling by liquid chromatography mass spectrometry (LC-MS/MS). Initially lysates were subject to trypsin digestion. Then peptides were labeled with tandem mass tag (TMT) reagents in two overlapping 10-plex sets for relative quantification of proteome and phosphopeptides (Figure 2.2). After reverse phase chromatography, LC-MS/MS was directly performed, or fractions were enriched for phosphopeptides by immobilized metal affinity chromatography (IMAC) followed by LC-MS/MS. 10,131 proteins were identified, with 9002 detected and quantified in every sample; 29,140 phosphopeptides were identified, corresponding to 12,325 identified in every sample.

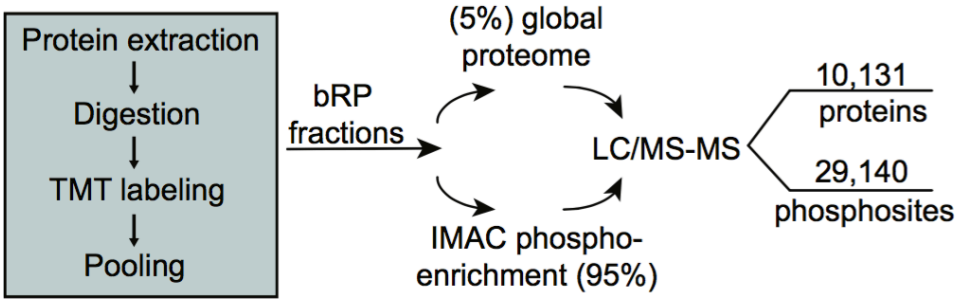

Figure 2.2. Workflow of LC-MS/MS to identify RIT1 and KRAS specific signaling.

Global phospho- and total proteomic profiling identify KRAS and RIT1-specific signaling significantly modulated by over-expressing wildtype and mutant KRAS and RIT1 in AALE human cell lines. TMT labeling, and protein enrichment were followed by LC-MS/Mass Spectrometry. (Courtesy of Alice Berger, Proteomic analysis performed by the Proteomics Core at the Broad Institute)

The novelty of this approach is that this is an unbiased study to interrogate RIT1 signaling. As opposed to previous studies, this assay does not rely upon the homology to RAS proteins to inform potential effector proteins. Protein profiling can be used to determine the similarities and differences of RIT1 and KRAS specific signaling in epithelial cells. Additionally, I interrogated if RAS proteins can form heterodimers. Specifically, I will investigate if KRAS and NRAS have the ability to form heterodimers with direct binding assays.

2.2 RESULTS

Using IP/MS data generated by the Berger lab my bioinformatic analysis suggests that NRAS may be a putative binding partner, and physically interact with KRAS in AALE epithelial cells (Figure 2.3A). As a preliminary validation of the dataset, a KRAS peptide was enriched, as would be expected with Flag-KRAS^{WT} pulldown.

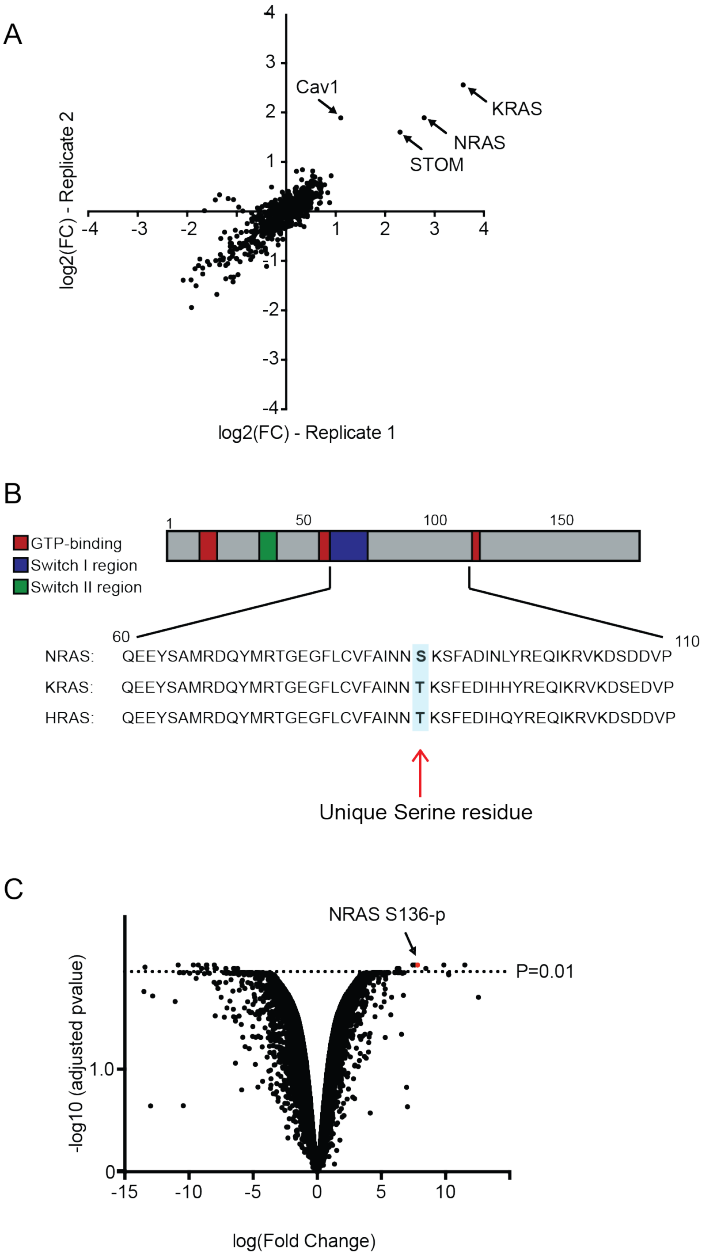

Figure 2.3. Global proteomic profiling data reveals NRAS as a KRAS interactor.

A) IP/MS data indicated that a NRAS interacted with KRAS in the $KRAS^{WT}$ overexpression in AALE (immortalized trachea-bronchial epithelial) cells. Phospho-proteomic data revealed NRAS phosphorylation at residue Serine 136 was increased as a result of wildtype KRAS over-expression *in vitro*. A) and B) Normalized to Renilla control. C) Unique NRAS peptide identified in wildtype LC-MS/MS mass spectrometry.

As previously stated, RAS proteins have ~80% significant homology[11]. Beneficially, upon Flag-KRAS^{WT} pulldown, there was enrichment for a unique peptide that mapped specifically to NRAS but not to KRAS or HRAS (Figure 2.3B). NRAS contains a Serine at residue S87 instead of a threonine, enabling specific identification of NRAS in the immunoprecipitated proteins. This indicates a putative KRAS-NRAS complex in human lung epithelial cells. It should also be noted that other peptides were identified that could map to either NRAS or KRAS. Additional phospho-proteomic analysis in the same cell line revealed NRAS phosphorylation at residue Serine 136 was increased as a result of wildtype KRAS over-expression (Figure 2.3C). Phosphorylation of S136 is a previously uncharacterized NRAS phosphorylation site.

Stomatin (STOM) and Caveolin1 (Cav1) were identified as potential KRAS binding partners, in addition to NRAS (Figure 2.3A). Both STOM and Cav1 both undergo farnesyl modification, which anchors the protein into the plasma membrane; both STOM and Cav1 contain a polybasic stretch of amino acids[74,75]. STOM is an integral membrane protein, and has been previously demonstrated to form homodimers[75,76]. The detection of these additional proteins which localize to the plasma membrane further raises the possibility that KRAS may interact with these proteins in lung epithelial cells.

Based upon the possible interaction of NRAS and KRAS, I hypothesized that like wildtype KRAS, wildtype NRAS might inhibit the progression of mutant lung adenocarcinoma. If so, we would expect there to be a selection against NRAS expression in *KRAS*-mutant lung tumors. To understand whether human tumors undergo selection for loss of NRAS expression, we analyzed gene expression and mutation data from The Cancer Genome Atlas project[2]. Data indicates that *NRAS* mRNA expression was modestly lower, yet statistically significant, in *KRAS*-mutant lung

adenocarcinomas compared to *KRAS* wildtype tumors (Figure 2.4). This is similar to the observation that wildtype KRAS is lost in human patients[63].

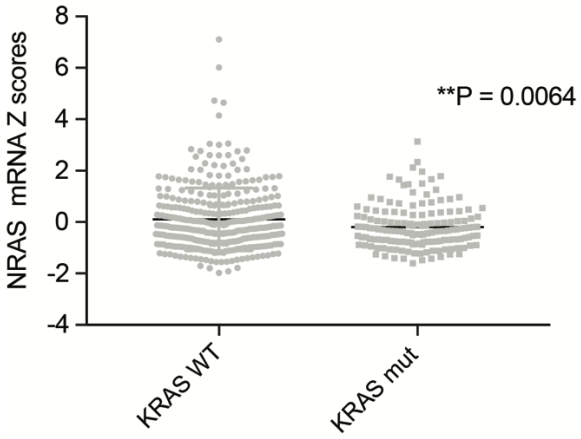

Figure 2.4. *NRAS* mRNA expression is downregulated in *KRAS*-mutant lung adenocarcinoma.

Analysis of TCGA data reveals *NRAS* mRNA expression is decreased in *KRAS*-mutant human lung adenocarcinoma samples (TCGA data form cBioPortal)

Summary of SEC with human recombinant proteins

Size exclusion chromatography (SEC) was performed to investigate the ability of KRAS and NRAS to physically heterodimerize. By using size exclusion chromatography, I have been able to resolve RAS monomeric fractions of his-RAS recombinant proteins. Expression plasmids containing human recombinant proteins of the catalytic G-domains (residue 1-167) of KRAS and NRAS with N-terminal his-tag were synthesized. Initially, the buffer was loaded with GDP. Initial expression and purification were successful and yielded his-KRAS^{WT} and his-NRAS^{WT}. His-tagged KRAS successfully purified as a monomer. Unfortunately, GDP bound his-NRAS did not elute from the SEC column as a stable monomer (Figure 2.5A-E).

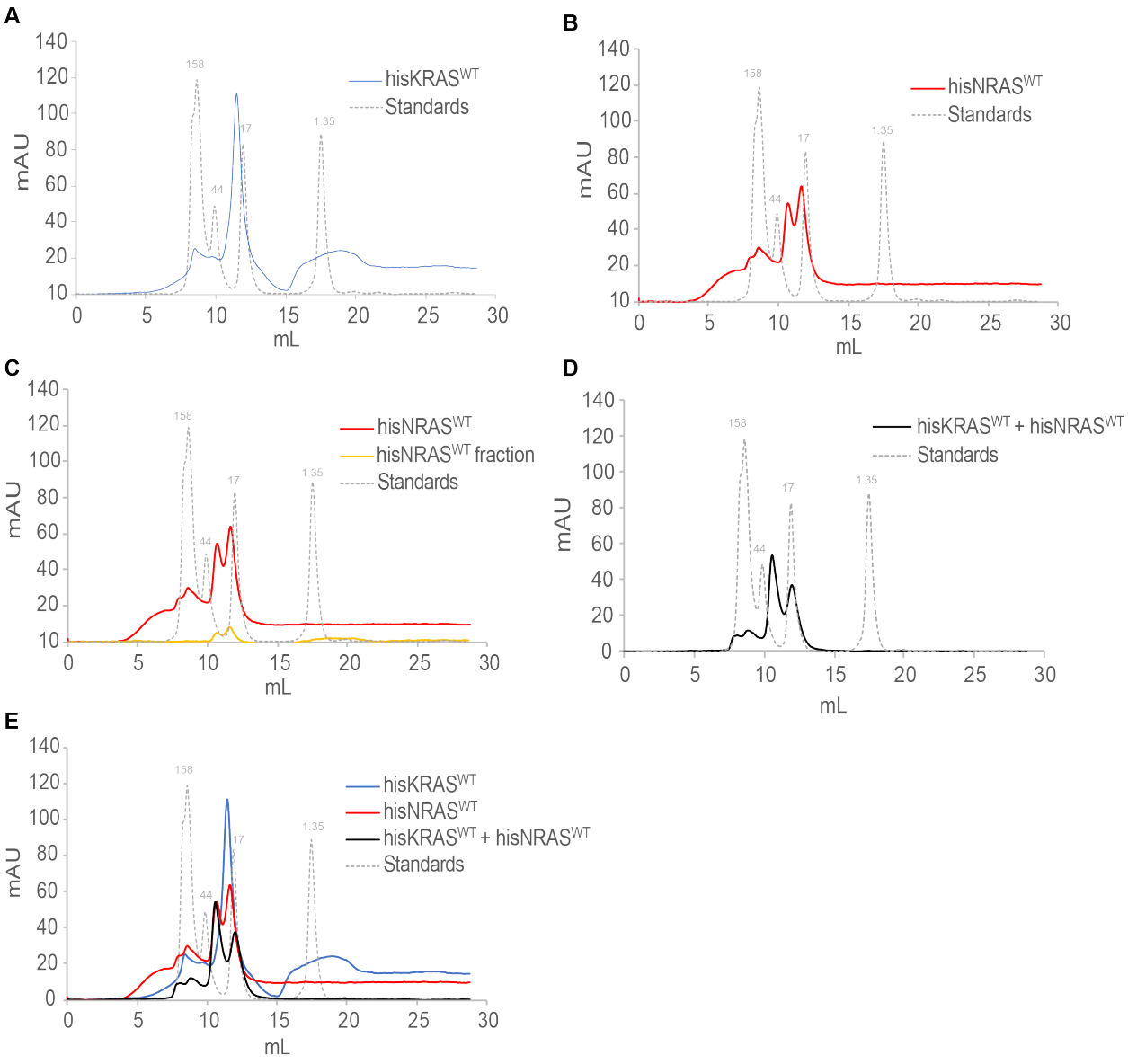

Figure 2.5. Size exclusion chromatography of his-KRAS^{WT} and his-NRAS^{WT} human recombinant proteins.

A) Size exclusion chromatograph of human recombinant his-KRAS^{WT}. B) Size exclusion chromatograph of human recombinant his-NRAS^{WT}. C) Size exclusion chromatograph of his-NRAS^{WT} monomeric fraction from (B). D) Size exclusion chromatograph of human recombinant his-KRAS^{WT} plus his- NRAS^{WT}. E) Overlay of graphs A, B, and D.

His-tagged $NRAS^{WT}$ eluted from the SEC column at two molecular weights. Rerunning the higher molecular weight over the SEC column yielded fractions with the same profile as the initial run at a lower, diluted, amplitude (Figure 2.5B). This indicates that his-NRAS recombinant protein was in dynamic equilibrium between monomeric and dimeric fraction. Unfortunately, since his-NRAS did not resolve as a monomer, the SEC assay was unable to distinguish between a NRAS homodimer and a putative KRAS-NRAS heterodimer (Figure 2.5E).

In order to overcome this challenge, I cloned the human recombinant RAS proteins to have a tag with a larger molecular weight, to allow for resolution during size exclusion chromatography. The MBP tag is approximately 41kDa. MBP-RAS recombinant proteins which express and fractionate at higher molecular weights than his-RAS proteins, ~63kDa compared to ~22kDa respectively. MBP-RAS^{WT} recombinant proteins were successfully expressed and purified (Figure 2.6).

After purification, MBP-KRASWT fractionates at the expected molecular weight (Figure 2.7A-B). The peak at molecular weight over the 670 standards is a higher order oligomer as indicated by the SDS-PAGE gel (Figure 2.7C).

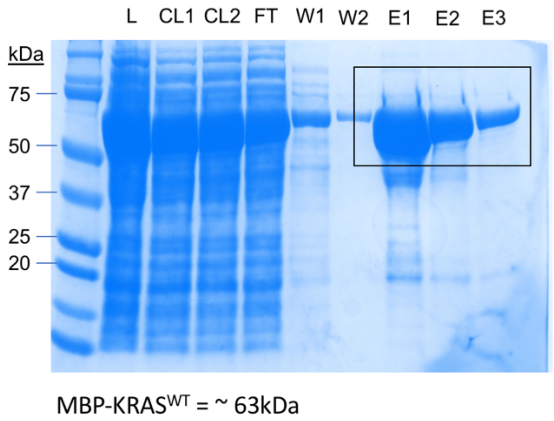

Figure 2.6. Expression of MBP-KRAS^{WT} human recombinant protein.

SDS-PAGE gel of samples taken during the purification process of human recombinant MBP-KRAS^{WT} protein. Expected size ~63kDa. {L=lysate; CL=cleared lysate; FT= flow through; W= wash; E= elution}

In future studies, I anticipate the ability to resolve RAS homodimers from putative RAS heterodimers, by combining a his-RAS protein with the appropriate MBP-Ras protein; future experiments would combine MBP-NRAS^{WT} with his-KRAS^{WT}, or MBP-KRAS^{WT} with his-NRAS^{WT}. In order to perform SEC, it is imperative to have a purified protein of both MBP-NRAS^{WT} and his-KRAS^{WT} of high quality. Unfortunately, while repeating the expression and purification process his-KRAS^{WT} was not visible in the elution lanes (*Data not shown*). After purification, the SDS-PAGE gel for his-KRAS^{WT} depicted a protein at the expected size washing off the column prior to the elution step, indicating a weak interaction. Therefore, it was concluded that the protein expressed was not his-KRAS^{WT}.

Additionally, the protocol for human recombinant his-RAS protein expression needs to be optimized in order to consistently observe the protein robustly expressed after IPTG induction, and during the elution step in the purification process. An alternative approach would be to utilize a yeast surface expression vector to interrogate if the G-domains of KRAS and NRAS can bind.

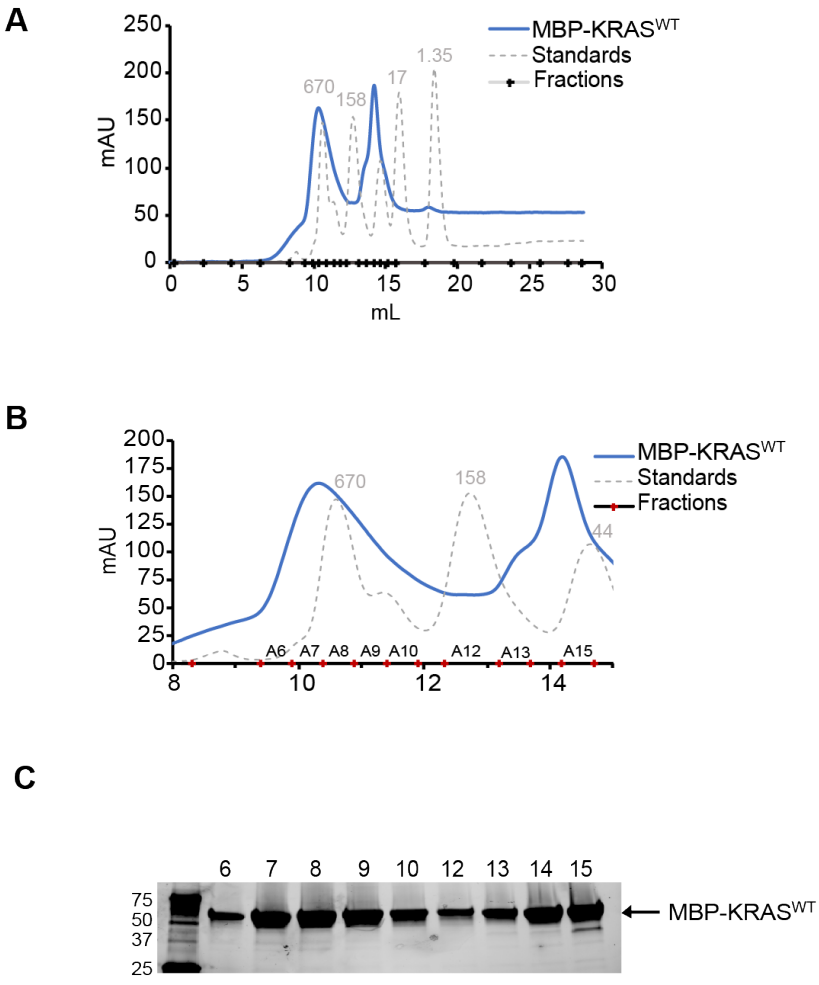

Figure 2.7. Human recombinant MBP-RAS expresses and is stable.

A) Size exclusion chromatography of MBP-KRAS^{WT} bound to non-hydrolyzable GTP. B) Closer view of (A). C) SDS-PAGE gel of MBP-KRAS^{WT} fractions, labeled in (B). Expected size of MBP-KRAS^{WT} is ~63Da.

Summary of Co-Immunoprecipitation in human cells

As an alternative approach to validate the physical interaction of KRAS and NRAS, I performed co-immunoprecipitation assays in HEK293 cells. The purpose of this assay was to determine if KRAS and NRAS physically interact in human cells.

A Western blot was performed for in HEK293 cells for Flag and V5; Vinculin was the loading control. Using total cell lysate, I was able to confirm expression of Flag-KRAS, at the expected size of ~21kDa (Figure 2.8A). The Flag antibody was used for immunoprecipitation to pulldown Flag-$KRAS^{WT}$; I was able to confirm that the Flag expression was enriched in the samples containing Flag-$KRAS^{WT}$ after Flag immunoprecipitation.

Whole cell lysate confirmed correct expression of V5-$NRAS^{WT}$ at the expected size of ~25kDa (Figure 2.8B). There was a band at the expected size of 25kDa in the Flag-$KRAS^{WT}$ and V5-$NRAS^{WT}$. However, this result was challenged by an observable band in the immunoprecipitation negative control lanes, lacking V5-$NRAS^{WT}$, indicating the problem of significant cross-reactivity between Flag and V5 antibodies Therefore, I concluded that co-immunoprecipitation was not able to confirm the physical interaction of $KRAS^{WT}$ and $NRAS^{WT}$ in HEK cells.

Given the proposed transient and perhaps weak nature of Ras dimers in general[6,41], it is unknown if co-immunoprecipitation would be able to detect KRAS homodimers. In order to determine if co-immunoprecipitation could be used to interrogate KRAS homodimers, I transfected Flag-$KRAS^{WT}$ and V5-$KRAS^{WT}$ in HEK293 cells. Successful expression of Flag-$KRAS^{WT}$ and V5-$KRAS^{WT}$ was determined by Western blot with whole cell lysate (Figure 2.8A-B). After Flag immunoprecipitation, Flag expression was enriched in the samples containing Flag-$KRAS^{WT}$.

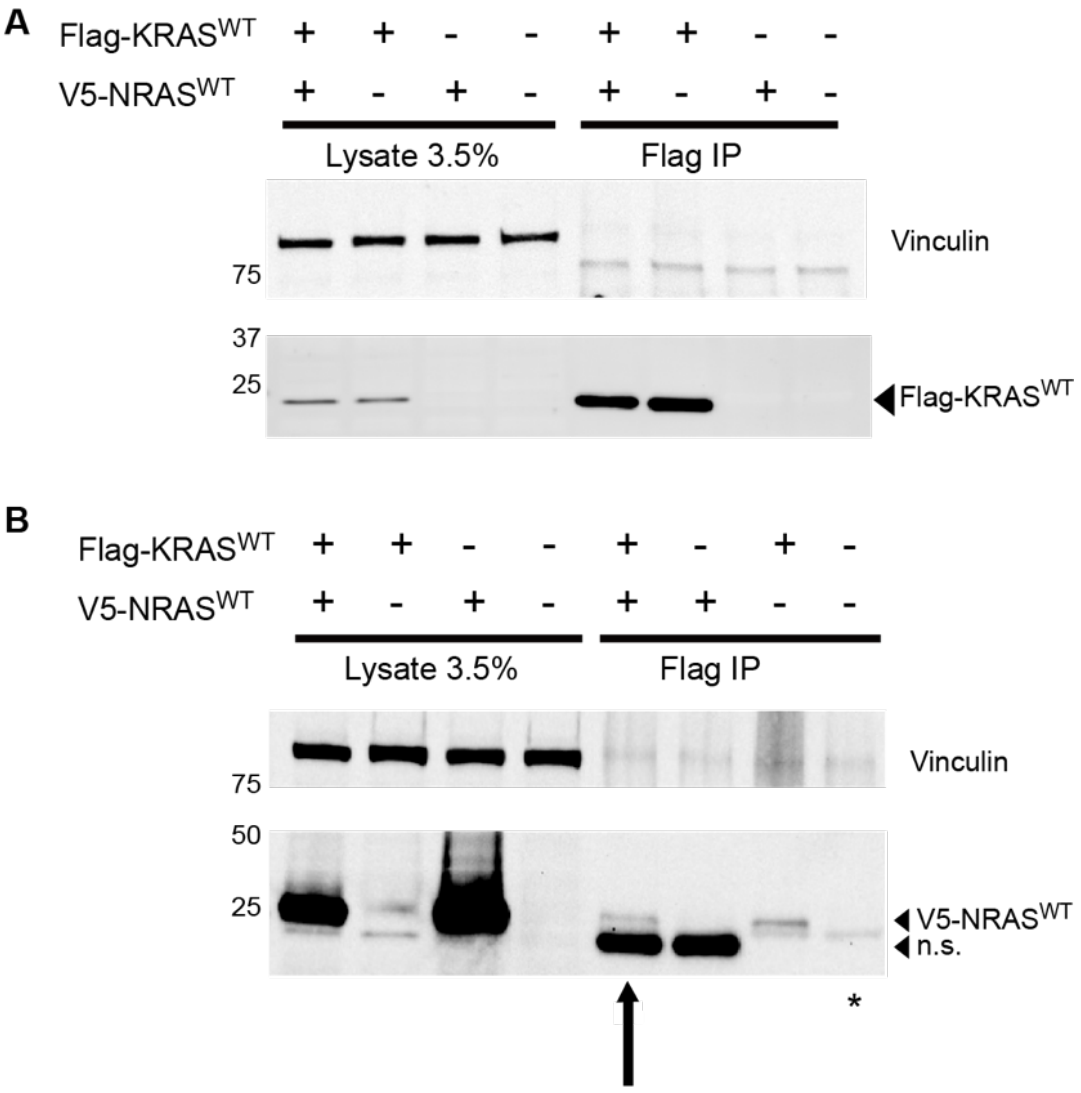

Figure 2.8. Co-immunoprecipitation results investigating putative KRAS/NRAS heterodimers

A) Immunoprecipitation results of Flag-KRAS^{WT} plus V5-NRAS^{WT}. Western blot with Flag antibody after Flag immunoprecipitation. 1000ug of whole cell lysate was loaded for Flag immunoprecipitation. B) Co-immunoprecipitation results of Flag-KRAS^{WT} plus V5-NRAS^{WT}. Western blot with V5 antibody after Flag immunoprecipitation. 1000ug of whole cell lysate was loaded for Flag immunoprecipitation. (*) symbol indicates the negative control lane.

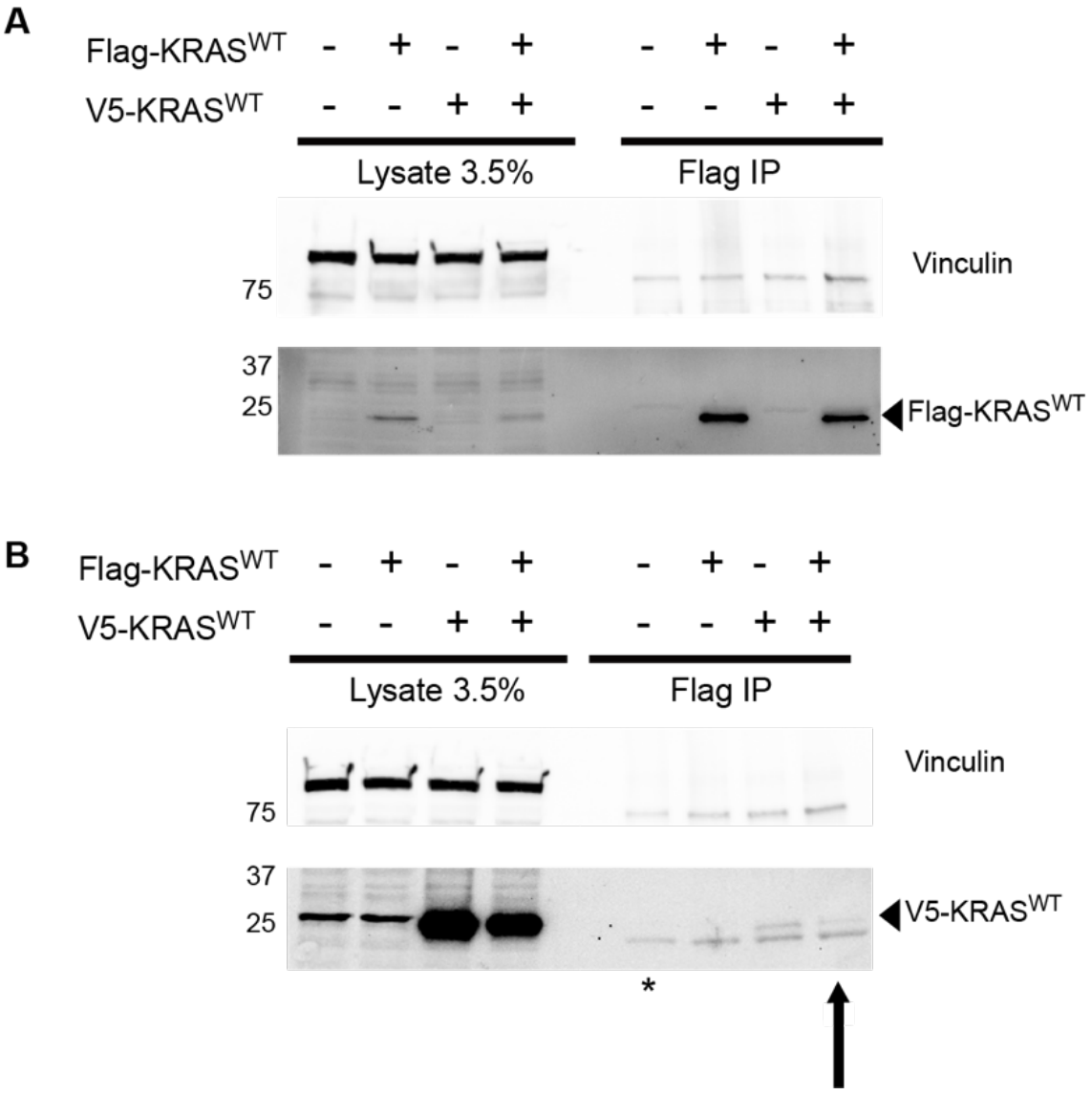

Figure 2.9. Co-immunoprecipitation results to detect KRAS homodimers.

A) Immunoprecipitation results of Flag-KRAS^{WT} plus V5-KRAS^{WT}. Western blot with Flag antibody after Flag immunoprecipitation. 1000ug of whole cell lysate was loaded for Flag immunoprecipitation. B) Co-immunoprecipitation results of Flag-KRAS^{WT} plus V5-KRAS^{WT}. Western blot with V5 antibody after Flag immunoprecipitation. 1000ug of whole cell lysate was loaded for Flag immunoprecipitation. (*) symbol indicates the negative control lane.

Despite the technical issues, there was no band at the expected size of V5-KRAS^{WT} (25kDa) in the Flag-KRAS^{WT} and V5-KRAS^{WT} lane (Figure 2.9B). Again, the problem of non-specific binding and cross-reactivity was observed as indicated by bands in the negative control lanes. Therefore, I concluded that co-immunoprecipitation as performed cannot detect KRAS homodimers in HEK293 cells.

These results do not negate the possibility that the endogenous NRAS may be able to form a complex with KRAS in human epithelial cells. This study utilized V5 tagged NRAS which did not replicate the design of the experiment which produced the preliminary data. In the original mass spectrometry data, endogenous NRAS was detected as a putative KRAS interacting protein upon pulldown with Flag-KRAS^{WT}. Additionally, in the future, buffer composition may be optimized based upon literature. Previous literature could also inform a positive control, which have previously been used for KRAS co-immunoprecipitation to validate the buffer composition, and the immunoprecipitation protocol. For example, OTUB1, a de-ubiquitinase, was confirmed by co-immunoprecipitation as a KRAS binding protein in HEK cells[77]. Additionally, this assay cannot rule out a tissue specific putative KRAS-NRAS heterodimer. Therefore, this assay could be repeated in AALE cells with a subsequent Western blot for endogenous NRAS. This setup will more closely replicate the preliminary data that collected the IP/MS and proteomics, which was the foundation for this research project.

A549 cells are human lung adenocarcinoma cells that harbor a G12S mutation[78]. NRAS was knocked down in A549 cells with shRNA targeted to NRAS. Lentiviral shRNA plasmids were purchased from SIGMA to target NRAS. A Western blot for NRAS was used to verify a decrease in NRAS protein abundance after treatment with shRNA targeting NRAS (Figure 2.10A). Additionally, Western blot confirmed the expression of V5-NRAS^{WT}.

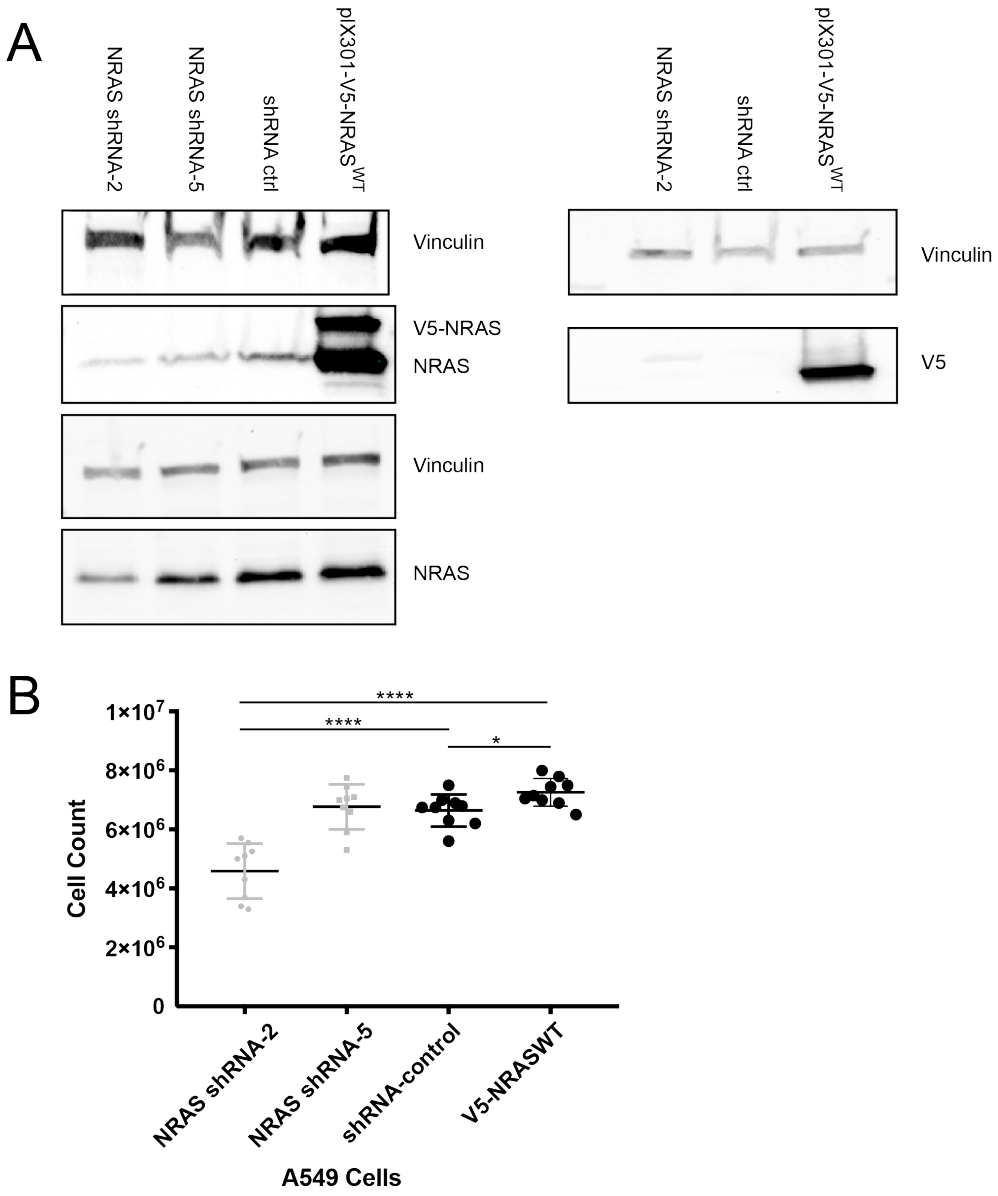

Figure 2.10. Reduced NRAS expression decreases proliferation in mutant KRAS lung adenocarcinoma cells.

A) Western blot to determine the expression of endogenous NRAS and V5-NRAS^{WT}. B) Proliferation assay of A549 cells after a decrease in NRAS expression by shRNA. Cells were seeded at 5x10^5 and counted after 13 days.

NRAS shRNA-2 produced a more effective knockdown of NRAS protein expression than NRAS shRNA-5. I hypothesized that NRAS may function similar to wildtype KRAS in mutant KRAS-driven lung adenocarcinoma. As a result, NRAS knockdown would cause an increase in A549 cells. However, cells with NRAS knockdown had a decrease in proliferation (Figure2.10B). Additionally, ectopic expression of V5-NRAS^{WT} indicated the opposite effect and increased the proliferation of A549 lung cancer cells. Future studies are necessary to further elucidate the role of wildtype NRAS in mutant KRAS-driven lung adenocarcinoma.

2.3 DISCUSSION

It is unknown if KRAS forms heterodimers with different RAS family members, and if this potential RAS/RAS heterodimer presents an opportunity for targeted therapeutics. Abrogating dimers may inhibit KRAS function in lung cancer patients harboring *KRAS*-mutations. Future studies could explore the possibility of RAS heterodimers. The majority of RAS studies have focused upon how RAS proteins function at the plasma membrane, however additional studies could focus on the functional effects of RAS proteins at endomembranes, like mitochondrial membranes.

Preliminary LC-MS/MS data identified NRAS as a putative KRAS binding partner. This study utilized biochemical and genetic systems to investigate the occurrence and role of putative KRAS/NRAS heterodimers in lung adenocarcinoma. The purpose of the study was to determine if the functional consequences of KRAS and NRAS heterodimerization is activating or inhibitory in lung cancer.

One of the challenges with proteomic profiling is that the lysates are subject to digestion and fragmented into peptides prior to LC-MS/MS detection and quantification. LC-MS/MS entails that the peptides are mapped back to specific proteins. The challenge is distinguishing proteins

with extensive sequence homology as there must be at least one unique peptide that specifically maps to only one protein. A technical challenge with performing immunoprecipitations with endogenous NRAS is the availability of an NRAS specific antibody. For example, the only NRAS-specific antibody identified in a study by NIH RAS Initiative study, was discontinued during this research project. The strength of proteomic profiling is the view of the global changes which occur.

Human recombinant proteins were expressed to perform size exclusion chromatography. Size exclusion chromatography was able to resolve stable his-tagged KRAS monomers. Unfortunately, his-tagged NRAS recombinant proteins were in dynamic equilibrium between dimers and monomeric fractions. A challenge with using size exclusion chromatography to resolve putative RAS heterodimers is that RAS proteins are the same molecular weight. Therefore, in order to confirm RAS heterodimers, the RAS proteins need to be tagged with epitopes which produce RAS proteins at sizes able to be resolved by size exclusion chromatography. Therefore, as conducted, this study was unable to distinguish between NRAS homodimers and a putative heterodimer. In the future, adding an MBP tag to one RAS protein would allow for better resolution between a RAS homodimer and a putative RAS heterodimer. Future work is needed to optimize the expression of recombinant RAS proteins to continue with this study.

Another challenge with using recombinant proteins to investigate RAS heterodimers is that KRAS/NRAS heterodimers may require additional proteins or factors, which size exclusion chromatography assay lacks. To overcome this challenge, I elected to perform immunoprecipitation. However, RAS homodimers have not been detected by co-immunoprecipitation and the proposed transient, and weak nature of RAS homodimers in general may present a challenge to using co-immunoprecipitation to detect RAS dimers[6,41]. Therefore, additional studies are necessary to detect physical interaction of KRAS with NRAS human cells.

More studies are necessary to confirm the observations that loss of NRAS causes a decrease in proliferation of mutant KRAS lung adenocarcinoma cells. Perhaps there is a threshold to the levels of NRAS where it exerts this effect. In the previous studies the increase in lung tumors was observed in NRAS-/- mice; however, the decrease in proliferation of colon cancer cells was a result of NRAS knockdown with shRNA. In the future, CRISPR could be used to produce a complete NRAS knockdown in A459 cells and additional other human lung adenocarcinoma cell lines.

The role of KRAS homodimers in driving KRAS-mutant lung adenocarcinoma has recently been discovered, but whether RAS proteins form heterodimers is unknown. Disrupting dimers can present a synthetic opportunity for previously ineffective therapeutics in RAS-driven cancers. Therefore, it is important to understand if RAS proteins heterodimerize, because it may present an opportunity for targeted therapeutics to become effective in ~30% of human tumors associated with RAS mutations.

Chapter 3. CHARACTERIZING THE RIT1- AND KRAS-REGULATED PROTEOME IN LUNG ADENOCARCINOMA

3.1 INTRODUCTION

RIT1 (RAS-like in all tissues) is a small GTPase in the RAS superfamily and contains similar features to the canonical RAS family members (ie. K-, H-, and N-RAS)[48,49]. Similar to most RAS proteins, RIT1 is ubiquitously expressed[48]. Novel RIT1 mutations were identified in patients with Noonan Syndrome. Noonan syndrome RIT1 mutations occur throughout the protein in the G1, switch I and switch II domains; the location of RIT1 mutation in Noonan syndrome contrast the location of mutations in HRAS found in Costello syndrome, which occur at residues G12, and G13 in the G1 domain[57,58].Additionally, RIT1 mutations have the ability to transform cells to harbor a cancer phenotype[52,65]. It was recently described that RIT1^{M90I} mutations disrupt the physical interaction between RIT1 and LZTR1. LZTR1 is a ubiquitin conjugating enzyme. RIT1^{M90I} mutants are unable to interact with LZTR1, causing RIT1 overexpression and increased downstream RAF/MEK signaling[52].

As previously stated, RIT1 contains a conserved G2 domain and effector region that are distinct from the RAS family[48,49]. The similar effector region to the RAS family suggests similar effectors. Yet the distinctions indicate that there are possibly unique effectors for RIT distinct from the RAS effectors. Comparing the proteomic profiles of RIT1 and KRAS proteomic profiles can elucidate the previously unknown downstream effects of RIT1 activation. The goal of this study was to use global proteomic profiling to determine the similarities and differences of Noonan syndrome and oncogenic RIT1 specific signaling, compared to oncogenic KRAS specific signaling in AALE, immortalized lung epithelial cells.

Previous studies have traditionally relied upon the homology between KRAS and RIT1 to study candidate signaling pathways. Given that a lot remains unknown about RIT1 biology, we elected to perform proteomic analysis to define RIT1 signaling pathways for therapeutic opportunities. We believe this is the first unbiased mapping of downstream RIT1 regulated signaling.

3.2 RESULTS

The canonical RAS signaling is downstream to the RAF/MEK/ERK cascade[12]. RIT1 also binds to C-RAF, inducing transcription of ERK target genes[52]. In order to determine if the downstream signaling cascade is regulated in the same way the following analysis was performed on AALE cells stably expressing the following: wildtype RIT1 or KRAS, $RIT1^{M90I}$, $KRAS^{G12V}$, $KRAS^{Q61H}$. Mutant $KRAS^{G12V}$, $KRAS^{Q61H}$, and mutant $RIT1^{M90I}$ all enhanced ERK phosphorylation relative to their wildtype counterpart (Figure 1.2). However, wildtype RIT1 also increased ERK phosphorylation, but wildtype KRAS suppressed ERK phosphorylation.

Proteome and phosphoproteome analysis revealed that the RIT1 mutant is very similar, yet distinct from the KRAS mutants. Proteome and phosphoproteome data from $RIT1^{M90I}$-expressing cells were highly correlated with $KRAS^{G12V}$ and $KRAS^{Q61H}$ profiles ($r = 0.70$-0.80 and 0.72-0.75 for proteome and phosphoproteome, respectively; Figure 3.1A). The high degree of correlation suggests that mutant $RIT1^{M90I}$ and KRAS mutants may have similar downstream consequences. As expected, $KRAS^{G12V}$ and $KRAS^{Q61H}$ proteomes and phosphoproteomes were highly correlated (proteome $r = 0.85$ and phosphoproteome $r = 0.79$). $KRAS^{G12V}$ and $KRAS^{Q61H}$ mutants are more similar to each other than to than to the $RIT1^{M90I}$ mutant. In contrast, the wildtype KRAS profile was the least correlated and most divergent of all the profiles. The wildtype KRAS downstream signaling profile is very different than the KRAS-mutant profiles or RIT1 profiles. However,

wildtype RIT1 more closely resembles the $RIT1^{M90I}$ profile than the wildtype KRAS resembles the mutant KRAS profiles (Figure 3.1A). A difference between KRAS and RIT1 is that over-expression of wildtype RIT1 can activate downstream oncogenic pathways, but over-expressing wildtype KRAS does not.

Certain proteins that were identified to be significantly modulated in LC-MS/MS proteome profiling were validated by Western blot. In LC-MS/MS data, FOSL1 had higher expression in mutant $RIT1^{M90I}$, $KRAS^{G12V}$, and $KRAS^{Q61H}$ cells compared to the wildtype or vector controls (Figure 3.1B). Western blots using independently derived AALE cell lines upheld a greater expression of FOSL1 in mutant cells compared to wildtype or vector controls. Additionally, LC-MS/MS identified TXNIP was one of top down-regulated proteins (Figure 3.1C). As expected, Western blot also confirmed a down-regulation of TXNIP expression in independently derived AALE cells. This demonstrates that protein expression changes identified by LC-MS/MS can be biochemically validated. Additionally, it demonstrates $RIT1^{M90I}$ may share a similar RAS-regulated mechanism to regulate FOSL1 and TXNIP.

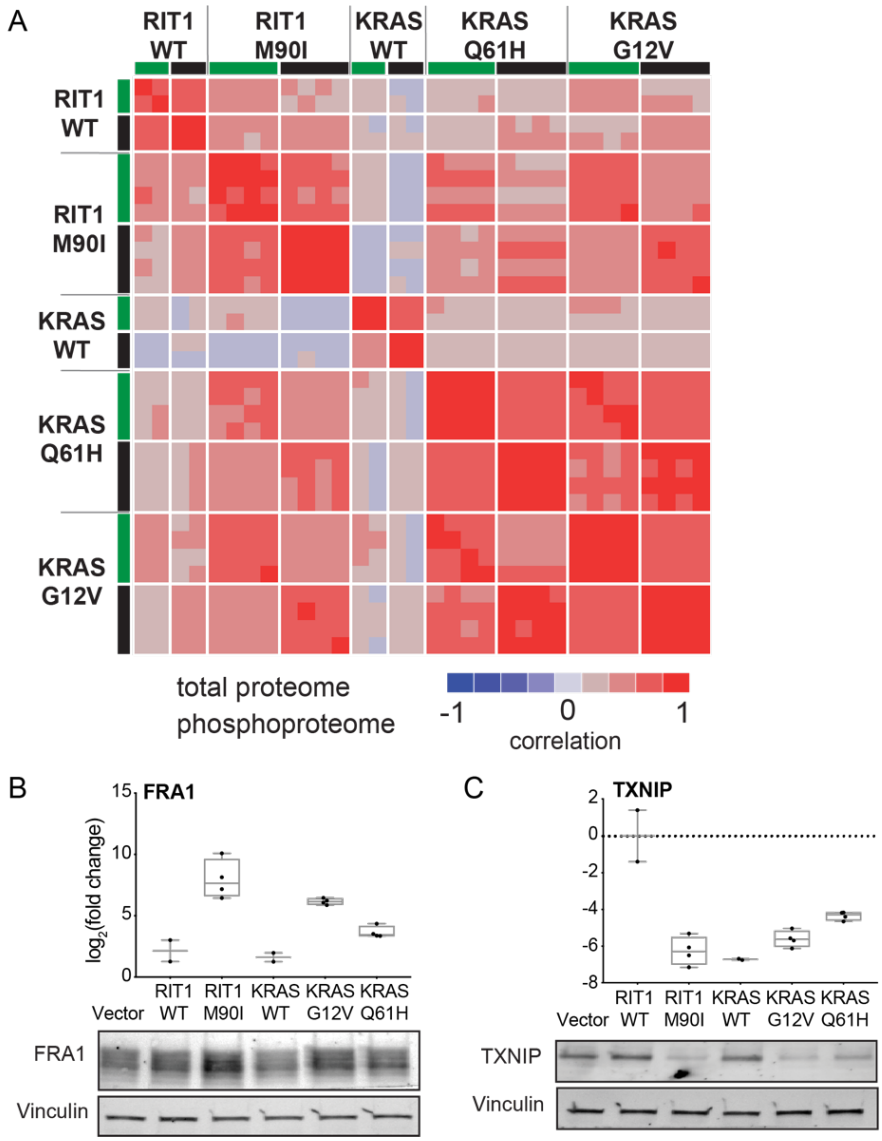

Figure 3.1. Proteomic profiling identifies global differences in RIT1 and KRAS mutants as determined by LC-MS/MS can be validated by Western blot.

A) Correlation heatmap showing correlations of RIT1 and KRAS proteome and phosphoproteome. Pearson and Spearman correlations of each proteome and phoshoproteome replicate to every other replicate. Phosphorylation sites were collapsed to the protein level by taking the median of all phosphorylation sites for each protein (Analysis performed by Alice Berger). B) LFC of FOSL1 and TXNIP as determined by LC-MS/MS and validated by Western blot. (Western blots for TXNIP and FOSL1 performed by Sitapriya Moorthi). C) LFC oF TXNIP as determined by LC-MS/MS and validated by Western blot (Western blots for TXNIP and FOSL1 performed by Sitapriya Moorthi).

KRAS and RIT1 mutants regulate EMT hallmark genes

Gene set overlap using MSigDB Hallmark pathway gene sets was performed. Analysis determines EMT is amongst the most differentially up-regulated gene sets in $KRAS^{G12V}$/$KRAS^{Q61H}$ and RIT^{WT}/$RIT1^{M90I}$ cell lines (Figure 3.2).

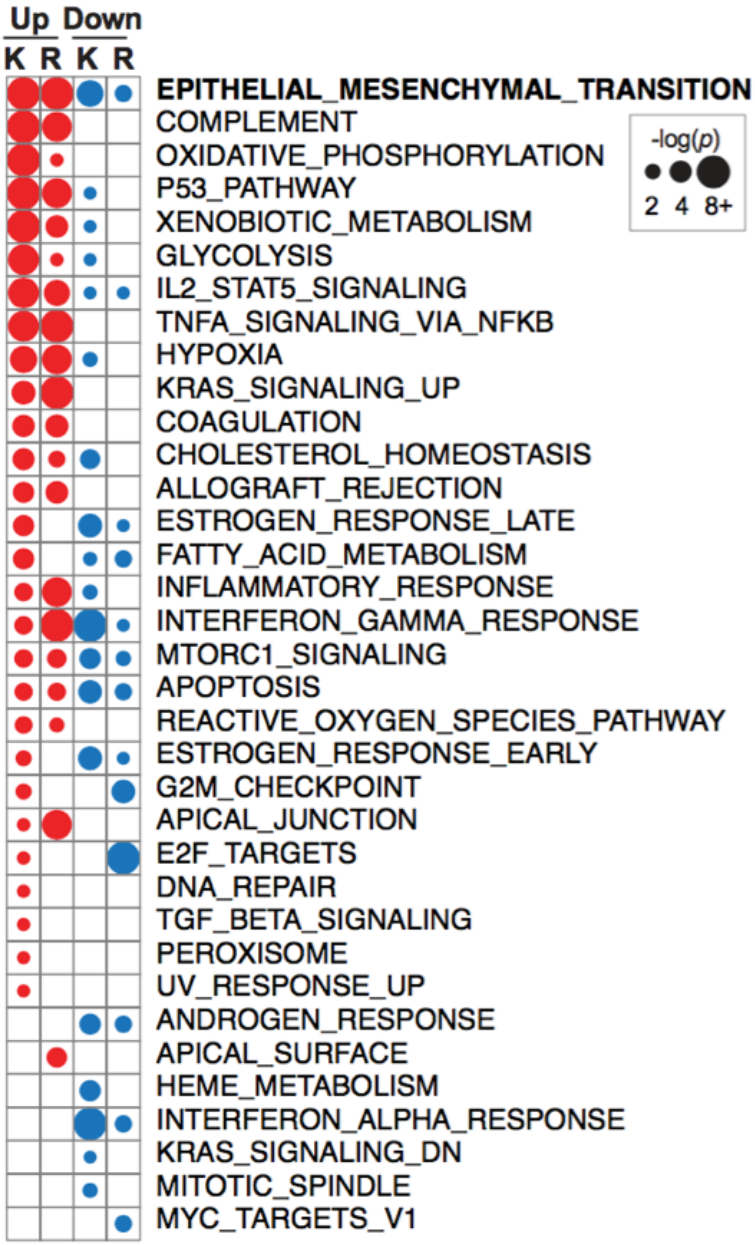

Figure 3.2. Gene set overlap analysis identifies epithelial-to-mesenchymal genes as a key signaling pathway in RIT1 and KRAS mutants.

Gene set overlap analysis of up-regulated (LFC >2) and down-regulated (LFC < -2) proteins using MutSigDB. "K" is the average of $KRAS^{G12V}$/$KRAS^{Q61H}$ cells; "R" is the average of $RIT1^{M90I}$/$RIT1^{WT}$. Circle size corresponds to the p-value as determined by MutSigDB. (Analysis performed by Alice Berger).

Previous literature has established that oncogenic KRAS promotes EMT[79]. The epithelial-to-mesenchymal transition is the process by which epithelial cells acquire mesenchymal properties, such as motility. Diverse signaling maintains the epithelial-to-mesenchymal transition. Analysis of the top10 genes up-regulated in EMT Hallmark gene set identifies many canonical markers of a mesenchymal transition (Figure 3.3A). Vimentin, N-Cadherin, and Fibronectin1 are canonical markers of mesenchymal cells; expression of these key mesenchymal genes in epithelial cells indicates an epithelial to mesenchymal transition[80]. Both $KRAS^{G12V}$, $KRAS^{Q61H}$, and $RIT1^{M90I}$ are capable of upregulating key EMT markers: Vimentin, N-Cadherin, and Fibronectin1 (Figure 3.3B-D).

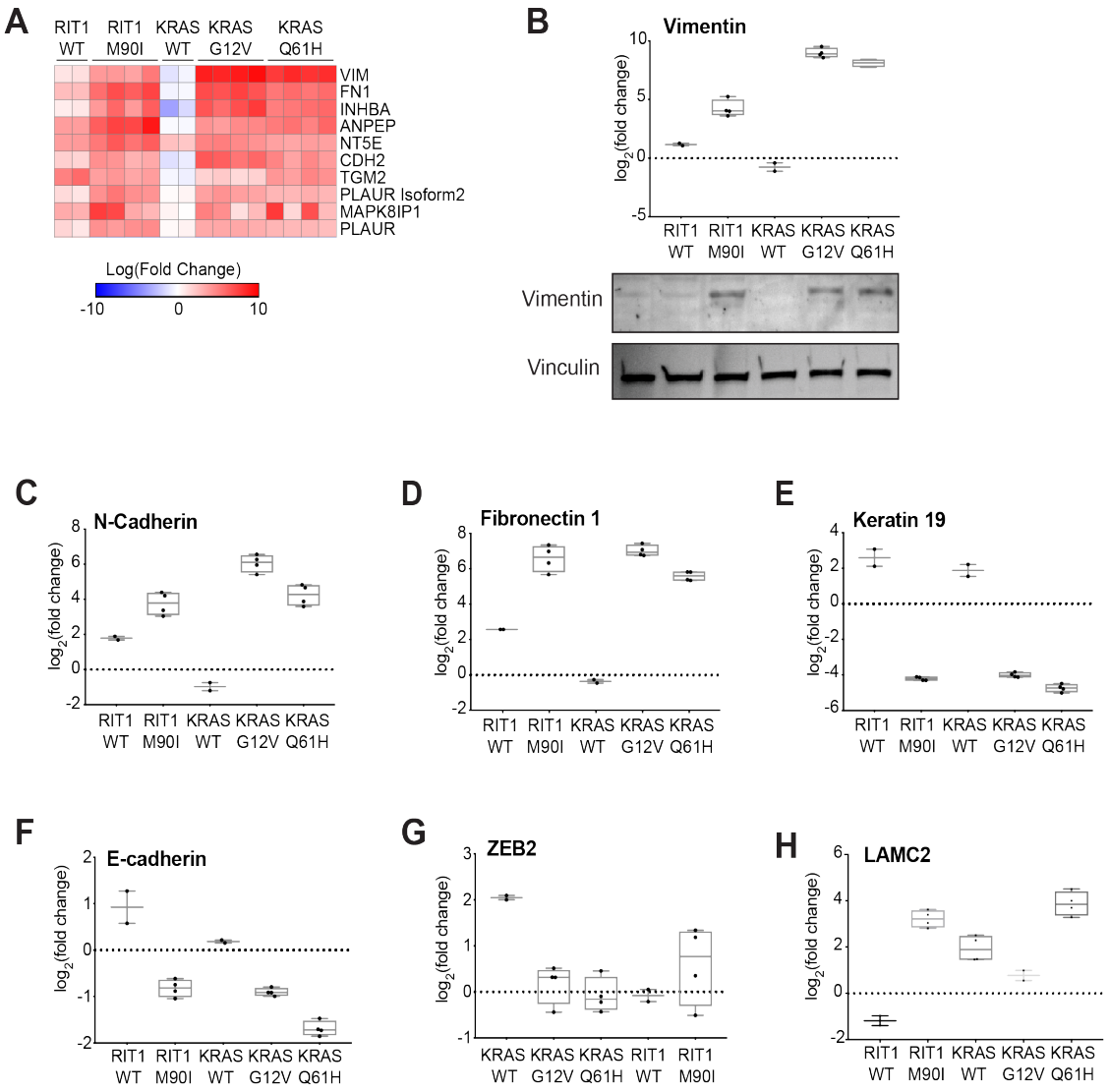

Figure 3.3. RIT1^{M90I} drives an epithelial-to-mesenchymal transition similar to KRAS mutants.

A) Heat map of the top ten up-regulated hallmark EMT proteins. Hallmark EMT proteins were identified from MutSig database. B) Log_2 fold change (LFC) of Vimentin as determined by LC-MS/MS (top) and validated by Western blot. Vimentin expression relative to control (luciferase-expressing AALE). (Western blots for Vimentin performed by Sitapriya Moorthi). C-G) LFC abundance of EMT marker genes, relative to control. H) LFC abundance of LAMC2 protein, relative to control.

Keratin19, is expressed in epithelial cells[81]. Keratin19 is down-regulated by mutants $KRAS^{G12V}$, $KRAS^{Q61H}$, and $RIT1^{M90I}$ (Figure 3.3E). The canonical EMT transcription factors Snail (SNA1) and Slug (SNA2) were not detected in the proteome analysis and may be expressed in quantities too small for detection. To my knowledge this is the first time it has been demonstrated that RIT1 promotes EMT in any cell type.

The proteomic profiling revealed other genes associated with EMT to also be modulated. E-cadherin is a marker of the epithelial cells and was shown to be down-regulated in the mutant $RIT1^{M90I}$ and mutant KRAS-mutant cells (Figure 3.3F). However, the down-regulation of E-cadherin protein abundance had a fold change less extreme than the up-regulation of key mesenchymal markers. Zeb2 protein abundance exhibited a unique pattern to the other EMT genes (Figure 3.3G). In previous studies, Laminin γ2 (LAMC2) was found to be up-regulated in lung adenocarcinoma metastatic cells, and expression of LAMC2 was found to be highly correlated with vimentin expression[82]. LAMC2 was upregulated in mutant KRAS and mutant $RIT1^{M90I}$-expressing cells (Figure 3.3H). Wildtype RIT1 phenocopied mutant $RIT1^{M90I}$ and mutant KRAS rather than wildtype KRAS. This is another instance of when the functional effects of wildtype RIT1 signaling diverges from wildtype KRAS signaling.

Oncogenic KRAS and RIT1 suppress MHC class I

Major histocompatibility complex (MHC) proteins were among the most suppressed proteins by mutant KRAS and $RIT1^{M90I}$ cells. Class I MHC proteins HLA-A, HLA-B, HLA-C, and HLA-F were dramatically down-regulated by $KRAS^{G12V}$, $KRAS^{Q61H}$, and $RIT1^{M90I}$ (Figure 3.4A-C). Observing the total proteome of $KRAS^{G12V}$ and $KRAS^{Q61H}$ reveals a striking down-regulation of the group of HLA proteins (Figure 3.4D-E).

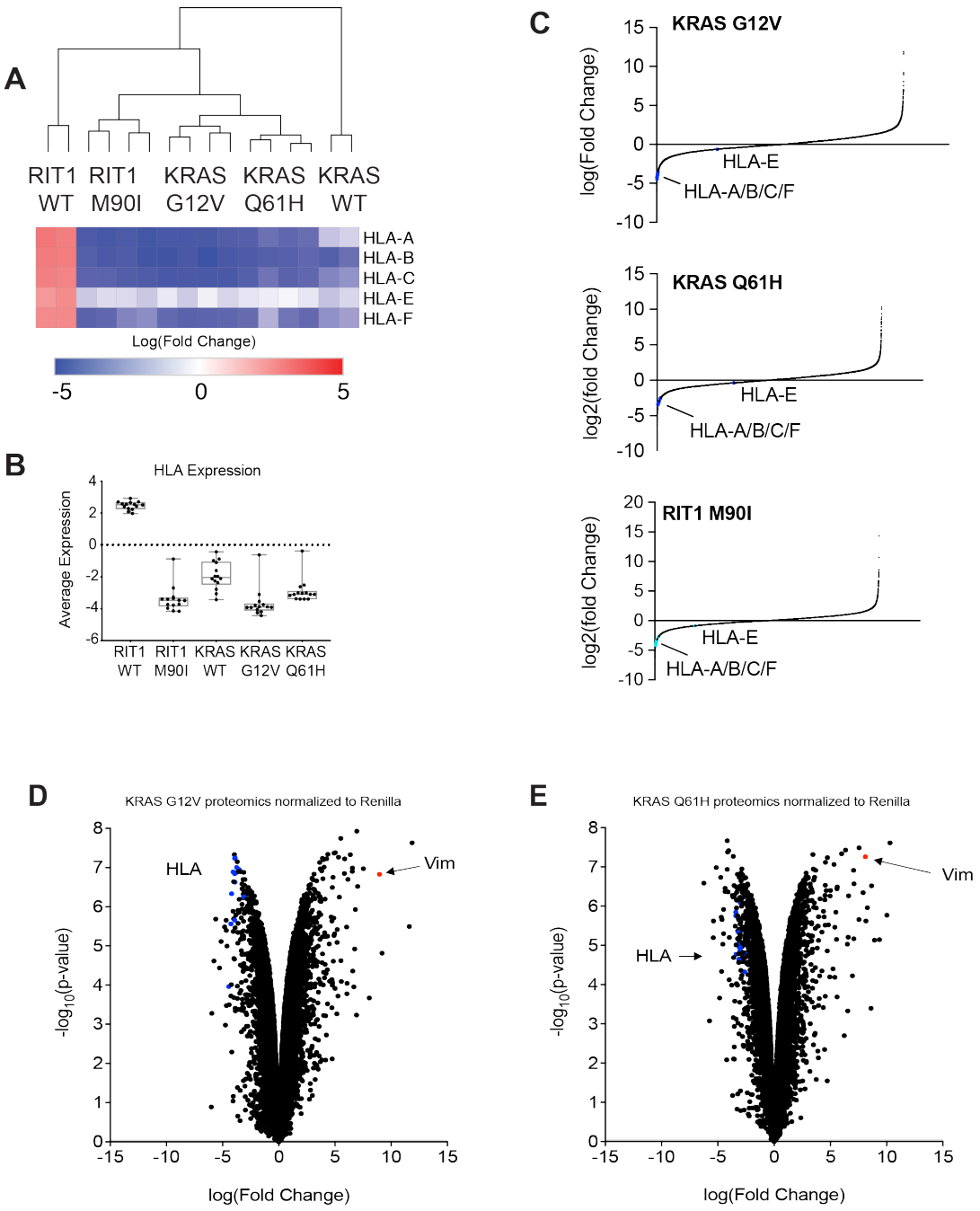

Figure 3.4. HLA proteins are down-regulated by RITM90I and KRAS mutants.

A) Heatmap of HLA protein abundance in each global proteome replicate.as determined by LC-MS/MS. B) LFC of HLA-A protein abundance, relative to control. C) Rank plot of all protein abundance changes in $KRAS^{G12V}$ cells. D) Total proteome of $KRAS^{G12V}$, normalized to control. HLA proteins and Vimentin labeled. E) Total proteome of $KRAS^{Q61H}$, normalized to control. HLA proteins and Vimentin labeled.

There is increasing interest in understanding the role of the immune system in cancer evolution. Supporting that notion, it is important to understand how HLA expression modulates metastatic *KRAS*-mutant lung adenocarcinoma.

B2M is another MHC class complex protein, whose expression loss is associated with resistance to immunotherapy[83]. Similar to HLA proteins, a dramatic loss of B2M expression was observed in $KRAS^{G12V}$, $KRAS^{Q61H}$, and $RIT1^{M90I}$ mutant cells (Figure 3.5A-B). In order to determine if this B2M down-regulation is observed in patient samples, I analyzed gene expression and mutation data from The Cancer Genome Atlas project[2]. Data indicates that *B2M* mRNA expression was modestly lower, yet statistically significant, in *KRAS*-mutant lung adenocarcinomas compared to *KRAS* wildtype tumors (Figure 3.5C). This is consistent with human tumors selecting for loss of B2M expression, but additional functional data is needed.

Other proteins with a similar expression patter to the HLA proteins may inform a possible mechanism of HLA suppression. Another protein with a similar expression pattern to the HLA proteins is PSMB9 (Figure 3.5D). PSMB9 (also known as LMP2) is a proteasome subunit. Loss of PSMB9 correlated with loss of HLA expression (Figure 3.5E). It has been previously demonstrated that a decrease of PSMB9 expression linked to a decrease of MHC proteins after oncogenic transformation[84]. Additional work is necessary to elucidate the mechanism of mutant $RIT1^{M90I}$ and mutant KRAS-driven suppression of MHC class I proteins.

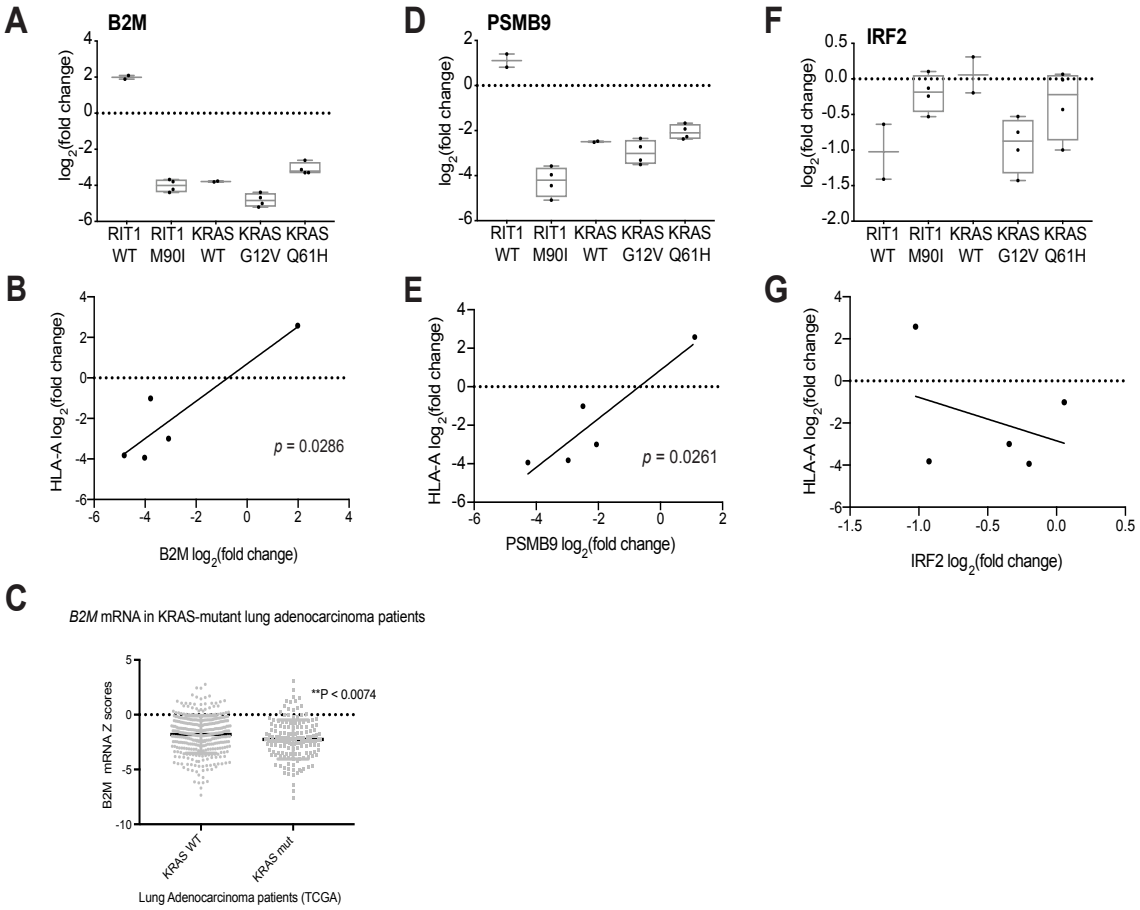

Figure 3.5. Class I MHC complex proteins correlate with HLA protein expression.

A) LFC of B2M protein abundance as determined by LC-MS/MS, relative to control. B) LFC of PSMB9 protein abundance as determined by LC-MS/MS, relative to control. C) LFC of IRF2 protein abundance as determined by LC-MS/MS, relative to control. D) Correlation of protein levels for B2M and HLA-A across each cell line. E) Correlation of protein levels for PSMB9 and HLA-A across each cell line. F) Correlation of protein levels for IRF2 and HLA-A across each cell line. G) Analysis of TCGA data reveals *B2M* mRNA expression is increased in *KRAS*-mutant human lung adenocarcinoma samples (TCGA data form cBioPortal)

It is challenging to explain the mechanism underlying the changes in HLA protein abundance. There observed changes in IRF2 protein abundance does not correlate with changes in HLA protein abundance across (Figure 3.5F-G) was there a difference which correlated between IRF2 and HLA-A protein abundance. Additionally, there were no transcriptional differences in upstream regulators of MHC class I, NLRC5 and IRF1(3.6A-B).

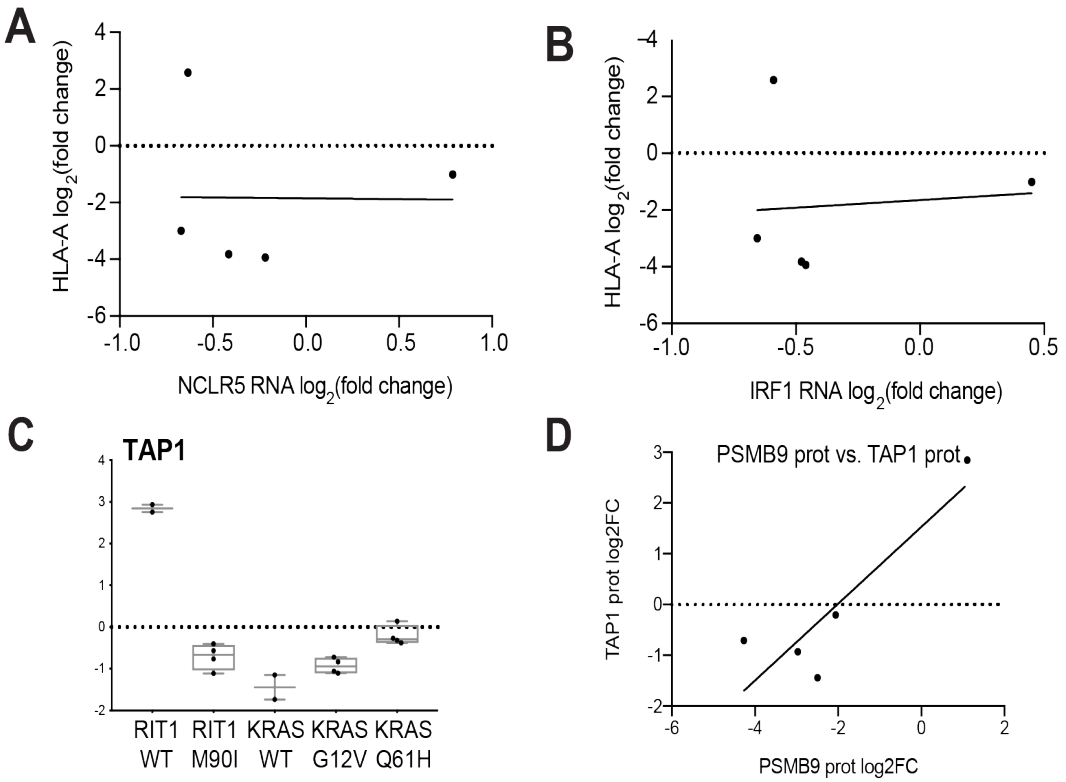

Figure 3.6. Understanding loss of class I MHC complex

A) Correlation for *NCLR5* RNA levels and HLA-A protein abundance across each cell line (Transcription analysis performed by April Lo). B) Correlation for *IRF1* RNA and HLA-A protein abundance across each cell line (Transcription analysis performed by April Lo). C) LFC of TAP1 protein abundance as determined by LC-MS/MS, relative to control. D) Correlation of protein levels for PSMB9 and TAP1 protein abundance across each cell line

It was concluded that the down-regulation of HLA proteins is not an artifact of lentiviral transduction as the $RIT1^{WT}$ cells maintained or increased HLA expression relative to the vector control (Figure 3.4A).

TAP1 has a similar expression pattern to the HLA proteins (Figure 3.6C). Loss of TAP1 correlates with loss of PSMB9 protein abundance (Figure 3.6D). PSMB9 and TAP1 are located adjacent on chromosome 6[85]. Perhaps the mechanism is that the entire region is being down-regulated. Future work is necessary to understand the mechanism underlying the observed loss of HLA protein abundance.

Phosphoproteome profiling identifies differences and similarities in RIT1 and KRAS signaling

By identifying proteins with differential phosphorylation between $KRAR^{G12V}$/$KRAS^{Q61H}$ and $RIT1^{M90I}$, divergent RIT1 and KRAS functions can be identified. Gene set enrichment analysis filtered for key RAS signatures, illustrates that the expected pathways were up-regulated in mutant KRAS and $RIT1^{M90I}$ cell lines (Figure 3.7A). It is interesting that wildtype KRAS cells down-regulated key RAS signature pathways. This again supports the notion that wildtype KRAS has an inhibitory role in KRAS tumorigenesis. KRAS is downstream of EGFR. Interestingly, EGFR phosphorylation was significantly modulated by KRAS mutants but not $RTI1^{M90I}$ (Figure 3.7B). EGFR total protein abundance was increased in KRAS mutant samples.

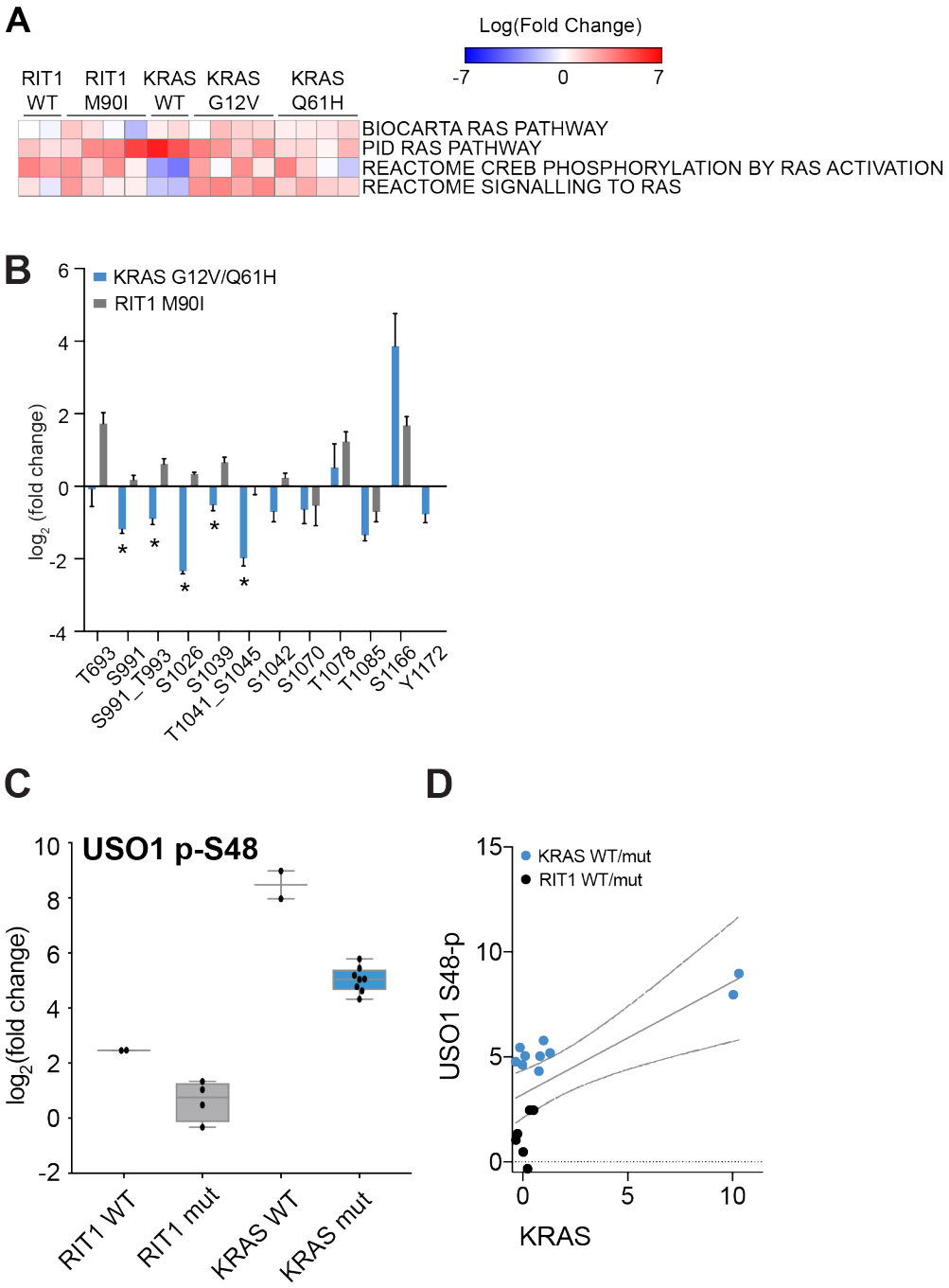

Figure 3.7. LFC of EGFR phosphorylation sites in RIT1-mutant versus KRAS-mutant cells.

A) Gene Set Enrichment Analysis (GSEA) identified pathways significantly modulated by *RIT1* or *KRAS* mutations. B) Differential EGFR phosphorylation D) USO linear correlation of S-48 phosphorylation and KRAS expression (Analysis performed by Alice Berger)

The following EGFR phosphorylation sites were significantly depleted in $KRAS^{G12V}$ and $KRAS^{Q61H}$ cells, but not $RIT1^{M90I}$: S991, S991/T993 double phosphorylation, S1026, S1039, T1041/S1045 double phosphorylation. It is unknown the mechanism of the depletion of EGFR phosphorylation at these specific sites. Future work could elucidate the feedback signaling between EGFR and KRAS.

Another protein which exhibited differential phosphorylation between RIT1 and KRAS expressing cells was USO1 phosphorylation at residue S48. There was significantly more phosphorylation in the wildtype KRAS-expressing cells compared to wildtype RIT1 cells (Figure 3.7C). There was a reduction in S48 phosphorylation abundance in the mutant RIT1 and mutant KRAS cells relative to its wildtype counterpart. USO1 phosphorylation at residue S48 correlated with KRAS expression (Figure 3.7D). In contrast, USO1 phosphorylation at residue S48 did not significantly change in the RIT1 samples (Figure 3.7C).

This study identified differences in EGFR and USO1 phosphorylation in mutant KRAS and $RIT1^{M90I}$ expressing cells. However, this was just a sample of the dataset. There are many differences that emerge between RIT1 and KRAS signaling that can be identified in the phosphoproteome. Future work can identify the differential phosphorylation of other proteins and the functional effects of specific residue phosphorylation in mutant KRAS and $RIT1^{M90I}$ expressing cells.

3.3 DISCUSSION

This study describes global proteomic and phosphoproteomic profiling of RIT1 and KRAS-regulated signaling. The unbiased approach identified similarities and differenced between RIT1 and KRAS-specific downstream signaling. One key observation is that mutant $RIT1^{M90I}$ seems to phenocopy wildtype RIT1. This supports the observation that oncogenic $RIT1^{M90I}$ functions in part

through increasing RIT1 abundance[52]. Unlike RIT1, the wildtype KRAS profile was very divergent or opposite to the mutant $KRAS^{G12V}$ and $KRAS^{Q61H}$ profiles. RIT1 can activate downstream RAF/MEK/ERK signaling when over-expressed. Therefore, RIT1 may not be regulated by GAPs in the same manner that keeps KRAS inactive.

One of the ways in which $RIT1^{M90I}$, $KRAS^{G12V}$, and $KRAS^{Q61H}$ are similar is that they induce EMT. EMT markers such as Vimentin, N-Cadherin and Fibronectin1 were all increased as a result of $RIT1^{M90I}$, $KRAS^{G12V}$, and $KRAS^{Q61H}$ expression in AALE epithelial cells. Additionally, epithelial marker such as Keratin19, and E-cadherin were down-regulated in $RIT1^{M90I}$, $KRAS^{G12V}$, and $KRAS^{Q61H}$ transformed epithelial cells. It was also observed that mutant KRAS and RIT1 led to a loss of HLA-A, HLA-B, and HLA-C expression. Another component of the MHC class 1 complex, PSMB9 was also down-regulated similar to the HLA proteins. It has been previously established that RAS proteins decrease MHC expression in cancer[86]. Additional assays in the same cell lines can, like flow cytometry and Western blot, can be performed to validate this observation. Future work will be necessary to elucidate the mechanism allow oncogenic RIT1 and KRAS to suppress MHC expression allowing for tumor evasion.

Phosphoproteome analysis revealed mutant RIT1 and mutant KRAS induced differential phosphorylation of EGFR. Future work will be necessary to determine the feedback regulation between KRAS and EGFR, and why KRAS but not RIT1 induces a decrease in EGFR phosphorylation. A technical challenge with proteomic profiling is the 1) quality of protein antibodies and 2) the availability of phosphorylation site-specific antibodies for subsequent biochemical validation of the key proteomic results. Orthogonal studies such as protein microarray utilize a more targeted set of established antibodies. This assay is an additional method to validate proteomic profiling and gather insight into oncogenic specific signaling[87].

This study presents an unbiased global proteomic and phoshoproteomic analysis to understand the similarities and differences between RIT1 and KRAS-specific signaling. It was confirmed that RIT1 can stimulate canonical RAS signaling cascades, such as RAF/MEK/ERK and PI3K. However, differences were identified as well. Future studies will follow up on this analysis to determine the possible functional effects in cancer and Noonan syndrome.

Chapter 4. CONCLUSIONS & FUTURE DIRECTION

We sought to identify genes important to, and identify sensitivities induced in lung adenocarcinoma subtypes. By combining proteomics and biochemistry, we were able to interrogate and identify the unique functional ramifications of RIT1 or KRAS signaling in lung adenocarcinoma.

4.1 PUTATIVE KRAS/NRAS HETERODIMERS

Previous studies have observed that RAS proteins have the ability to form homodimers, and KRAS homodimers have a functional role in promoting tumorigenesis. This study investigated if RAS proteins can form heterodimers, specifically if NRAS and KRAS interact in lung adenocarcinoma. While NRAS is a putative KRAS binding partner, it is inconclusive if NRAS and KRAS can from heterodimers. As part of this study, I designed an experiment to investigate the functional role of NRAS in mutant *KRAS*-driven lung adenocarcinoma *in vivo*. Although this study is ongoing, in data generated thus far, there appears to be a functional interaction between KRAS and NRAS in murine models of mutant KRAS (data not shown). This study describes a preliminary assay indicating that loss of NRAS in mutant KRAS lung adenocarcinoma cells, leads to a decrease in proliferation; conversely proliferation increases when wildtype NRAS is overexpressed in mutant KRAS lung cancer cells. Future work is necessary to determine if there is a tissue-specific functional role of NRAS in mutant KRAS lung adenocarcinoma.

While a unique NRAS peptide was detected in order to identify NRAS as a putative KRAS binding partner, additional studies are necessary to conclude if KRAS and NRAS physically interact. In this study, I performed size exclusion chromatography with human recombinant proteins. This study utilized the G-domain of RAS proteins and lacked the

hypervariable C-terminal region. Since NRAS was resolved as a monomeric and dimeric fraction, size exclusion chromatography was unable to distinguish between a NRAS homodimer, and a putative KRAS/NRAS heterodimer. This study utilized overnight IPTG induction at 16C. One possibility would be to vary the induction timeline and the competent cells. Future work will be to optimize the expression of MBP-RAS and his-RAS human recombinant proteins.

A limitation of size exclusion chromatography with human recombinant proteins is that additional cellular factors may be required to facilitate the physical interaction of KRAS and NRAS lacking in this experimental context. To overcome this limitation, I sought to perform co-immunoprecipitation with Flag-KRAS^{WT} and V5-NRAS^{WT}in HEK293T cells. Unfortunately, my studies proved inconclusive, and the experimental setup could be improved. The preliminary LC-MS/MS data which identified NRAS as a putative KRAS binding partner was performed in AALE cells. As AALE cells are immortalized epithelial cells, it cannot be ruled out that a KRAS/NRAS heterodimer may be a tissue-specific interaction. Nor can it be concluded that the V5-tag does not disrupt the putative KRAS/NRAS heterodimer.

Furthermore, it has been postulated in the literature of RAS homodimers, that RAS dimers may be transient and weak, rendering them difficult to detect. Previous studies reporting RAS homodimers utilize fluorescence-based proximity assays as evidence of RAS homodimers. Co-immunoprecipitation has not been reported for KRAS homodimers. Indeed, when I performed co-immunoprecipitation for Flag-KRAS^{WT} and V5-KRAS^{WT}, I was unable to detect KRAS homodimers. Therefore, even if KRAS/NRAS heterodimers occurred, they may be lost during the immunoprecipitation process. Future work would be to optimize the buffer composition, and immunoprecipitation protocol to detect KRAS homodimers as a positive control to determine if co-immunoprecipitation can resolve RAS homodimers.

4.2 CHARACTERIZING MUTANT RIT1 AND KRAS PROTEOME IN LUAD

This study utilized global proteome and phosphoproteome analysis to elucidate the similarities and differences between RIT1 and KRAS-specific signaling. Previous studies relied upon the homology between RIT1 and KRAS to identify putative RIT1 effector proteins, or downstream signaling cascades. Therefore, an advantage to this study was that it analyzed the entire global proteome for RIT1 effector proteins in an unbiased manner.

A challenge with validating the LC-MS/MS proteome and phosphoproteome profiles is the availability of protein antibodies. This study identified that, generally, EGFR phosphorylation at specific residues was decreased by KRAS mutants. However, of almost all of these phosphorylation sites lack a phospho-specific antibody, so we were not able to perform additional validation. Additionally, USO1 was identified to have differential phosphorylation, but unfortunately, USO1 protein lacks a phospho-specific antibody. A fluorescence-based protein microarray is an alternative assay to proteome profiling[87]. The benefit to protein microarrays is the ability to do downstream validation assays with quality antibodies for protein expression. While protein microarrays focus proteomic analysis by analyzing a smaller subset of the proteome, the antibodies used in the protein microarray are validated to be of high quality; this facilitates the biochemical validation of the protein microarray. Subsequently, certain key signaling pathways identified by the microarray can be validated by Western blot and immunohistochemistry tissue staining. Additionally, the results of the microarray can be functionally validated by knocking down the detected downstream markers of RIT1 activation and assaying for proliferation (Ki67 staining) and ERK phosphorylation.

Chapter 5. MATERIALS AND METHODS

5.1 PLASMIDS

The cDNA of the following RAS constructs in pDONR plasmids were obtained from NIH RAS initiative: KRAS4B^{WT}, KRAS4B^{G12V}, KRAS4B^{Q61H}, and NRAS^{WT}. The plasmid pLX-TRC313-Flag-*KRAS^{WT}* was previously generated in the Berger lab. N-terminus tagged Flag-*KRAS^{WT}* cDNA sequence was amplified using PCR; the primers were designed to to amplify the Flag-*KRAS^{WT}* amplicon for subsequent Gateway cloning. The LR reaction The LR reaction (ThermoFisher) was A plasmid expressing N-terminal tagged V5-NRAS^{WT} was generated by performing an LR to introduce NRAS^{WT} constructs (p-DONR-NRAS^{WT}) into pcDNA3.1-V5-Dest (ThermoFisher). An LR reaction was performed to introduce Flag-KRAS^{WT} constructs (p-DONR-KRAS^{WT}) into pcDNA3.1-V5-Dest.

Lentiviral plasmids MISSION shRNA plasmids, which target human NRAS, were ordered (Millipore SIGMA).

The sequence of NRAS shRNA - #2 (TRCN0000300441) is:

CCGGGAAACCTGTTTGTTGGACATACTCGAGTATGTCCAACAAACAGGTTTCTTTTG.

The sequence of NRAS shRNA #5 (TRCN0000300367) is:

CCGGCAAGAGTTACGGGATTCCATTCTCGAGAATGGAATCCCGTAACTCTTGTTTTG.

The pDONR-NRAS^{WT} plasmid was received from the NIH RAS initiative. The V5 epitope tag was introduced by PCR with primers to generate V5-NRAS^{WT} amplicon. Next, the pDONR-V5-NRAS^{WT} plasmid was generated by performing a BP reaction (Thermo Fisher Scientific) with the V5-NRAS^{WT} amplicon and pDONR-223; this was confirmed by sequencing. The lentiviral plasmid plX301-V5-NRAS was generated by performing a LR reaction to with pDONR-V5-NRAS^{WT} and empty plX301 backbone vector. The plasmid plX301-V5-NRAS^{WT} was confirmed

with sequencing.

5.2 Cell Line Generation & Proliferation Assay

Lentivirus expression:

On day 1, Lentivirus was created by plating $2x10^6$ HEK293T cells per 10cm plates. On day 2, lentivirus is transfected after diluting 1.5ug of plasmid delta8.9, 150ng VSV-G with 1.5ug of each lentiviral plasmid with OPTI-MEM (Thermo Fisher Scientific). The lentiviral plasmids were NRAS-shRNA-2, NRAS-shRNA-5 and plX301-V5-$NRAS^{WT}$. In a separate tube, a mix containing 9uL Fugene (Promega) and 36uL OPTI-MEM for each transfection and incubated for 5min at room temperature. Then 45uL of the Fugene/OPTI-MEM mix is added to each tube containing the plasmid/OPTI-MEM. After a 30min incubation, the mixture was dripped onto the 10cm plates. On Day 3, the media was changed to DMEM plus 30% FBS. On Day 4, the virus was harvested and frozen at -80C. The media was collected, centrifuged and the supernatant was collected.

Cell line generation:

A549 cells were counted and $5x10^5$ plated in 1 well of a 6WP. An extra well was seeded to be the no virus control. On day 2, the media was changed to contain 8ug/mL polybrene, and 300uL of virus was added to each well of the 6WP. On day 3, antibiotic selection started, and the media was changed to contain 2ug of puromycin. After 4 days of selection the non-virus control cells were dead and the cell lines were harvested. The cell lines were generated in replicate of 2 and combined when harvesting.

Proliferation assay:

On day 1, A549 cells were counted and 50,000 cells were plated into a 10cm plate in triplicate. After 13 days the cells were harvested and counted. This was performed three times

5.3 DNA TRANSFECTIONS, CELL LYSIS, AND WESTERN BLOT ANALYSIS

I transiently transfected pDest40-Flag-*KRAS*^{WT} and pcDNA3.1-V5-*NRAS*^{WT} into HEK293T cells. For individual transfections, 2000ng of each plasmid DNA (pDest40-Flag-*KRAS*^{WT} or pcDNA3.1-V5-*NRAS*^{WT}) was added to the Lipofectamine + optimum mixture for each well of 6WP. For co-transfections, 1000ng of pDest40-Flag-*KRAS*^{WT} and pcDNA3.1-V5-*NRAS*^{WT} were added to the Lipofectamine + optimum mixture. After 20min incubation, 100uL of each sample is dripped into each well of 6WP. As a transfection control I separately transfected in p-EGFP at the same total DNA concentration. Within 24-65hrs post transfection I harvested the cells for Flag immunoprecipitation. BCA normalization was performed. Primary antibodies were incubated overnight at 4C. Membranes were washed with TBS-T 3x5mL. Secondary antibodies were incubated for 1hr at room temperature. Membranes were washed with T 3x5mL of TBS-T. The membranes were washed and stored in PBS.

5.4 ANTIBODIES/IMMUNOBLOTTING

The primary antibody for Flag (14793S) is from Cell Signaling Technology. V5 (AB3792) primary antibody was from EmdMillipore/Sigma. The antibody to detect NRAS (F155) is from Santa Cruz Biotechnology. The vinculin (V9264) antibody was from Sigma Aldrich. The secondary antibodies were BrighStar700 anti-rabbit (Bio-Rad), IRDye800CW Goat anti-rabbit IgG and IRDye800CW Goat anti-mouse IgG from LI-COR. Primary antibodies were incubated overnight at 4C. Secondary antibodies were incubated for 1hr at room temperature. Proteins were visualized using the ChemiDoc MP Imaging System (Bio-Rad).

5.5 IMMUNOPRECIPITATION

Total cell lysate (1000ug) was the input for immunoprecipitation pulldown. The pre-conjugated Flag affinity gel (Sigma) was used for Flag immunoprecipitation according to manufacturer's protocol. Elution from the Flag beads was performed with 20uL of 2X SDS-Page elution buffer. 10uL of the elution sample was used in the Western blot for Flag, and the remaining sample was used in the Western blot for V5.

5.6 GENERATING RECOMBINANT PROTEIN EXPRESSION PLASMIDS

The Stoddard lab (Fred Hutch) previously generated and validated the human recombinant expression plasmid: pET15(HE). I designed the human recombinant protein to include only the catalytic G-domain of RAS proteins, lacking the hypervariable region (residues 1-167). The protein sequences for human KRAS (hKRAS) and human NRAS (hNRAS) were downloaded from ENSEMBL (Ensembl.org).

The expected size of human KRAS and human NRAS are both ~500bp. The final pET15(HE)-hKRAS and final pET15(HE)-hNRAS plasmids was synthesized by GENEWIZ.

Cloning MBP-RAS from his-RAS plasmid:

The sequences for KRAS and NRAS were cloned into the pMAL plasmid (New England BioLab), which is an MBP expression vector, in order to generate MBP-RAS. The molecular weight of MBP-Ras is ~63kDa. First, pET15(HE)-hKRAS and pET15(HE)-hNRAS were digested with NotI/NcoI restriction enzymes. The digested plasmids were run on an agarose gel to confirm digestion. The expected size of human KRAS and human NRAS are both ~500bp. The human KRAS and human NRAS were extracted from the gel by gel Extraction kit (Qiagen). The NotI/NcoI digested hKRAS was ligated into the NotI/NcoI digested pMAL vector, with 1uL of

Quick Ligase (New England BioLab). The ligation was similarly performed with insert NotI/NcoI digested hNRAS into the pMAL vector. The MBP-RAS plasmids were confirmed by NotI/NcoI double restriction enzyme digestion. 1mL sample taken when target optical density is lysed and run on SDS-PAGE gel to confirm the recombinant protein was expressed at the expected molecular weight.

5.7 Recombinant Protein Expression

Protein expression was based upon a previously established protocol by Stoddard Lab. The expression plasmid was previously generated in the Stoddard lab.

Expression plasmids were transformation in RIL competent cells. A his-KRAS^{WT} colony, and an MBP-NRAS^{WT} colonies were picked and put into individual 10mL overnight cultures of LB-Amp. The following morning the 10mL culture was put into 1L LB-Amp culture into a shaking incubator at 37C until optical density of 0.6-0.8 is reached. Subsequently, IPTG was added to a final concentration of 0.5mM IPTG for overnight induction, at 16C. To harvest the protein, 1L was centrifuged at 4000rpm for 30min at 4C. The supernatant was discarded, and the pellet was resuspended in ~30mL of PBS. The suspension was centrifuged again, and the supernatant was discarded, and the pellet was frozen at -20C.

5.8 Recombinant Protein Purification and Size Exclusion Chromatography

The following buffers were used:

His-RAS Buffer A – 20mM Tris pH 8.0; 5 mM MgCl2; 50mM NaCl; 5% glycerol; 20 uM GDP; 1mM DTT

MBP-RAS Buffer A – 20mM NaCl; 20mM Tris-HCl; 1mM EDTA; 1mM DDT (pH = 7.4 at 25C).

The bacterial pellet was resuspended in 30mL of Buffer A. After resuspension, additional Buffer A was added to a final volume of 50mL. The proteasome inhibitor, PMSF, (100uL of 100mM stock solution) was added before sonication. The sample was sonicated for lysis at 18W with a cycle of 30sec ON/ 30sec OFF repeated 5 times. A 10uL sample is taken (L = lysate). The sample was centrifuged at 16,000 rpm for 20min at 4C to clear debris. A 10uL sample of the supernatant is taken (CL = cleared lysate). Polyethyleneimine (PEI) was added to the samples to 0.02% w/v and the samples are incubated at 4C for 30min with gentle rocking.

IMAC purification: Based upon previously established protocol by Stoddard Lab

For subsequent IMAC purification, the samples are filtered through a column containing a 0.45um filter with gravity flow.

To purify his-RAS proteins contained 4mL of nickel resin (New England BioLabs) was added to the column and EtOH solution was allowed to gravity drip to a final resin volume of 2mL. Buffer A contained 20uM GDP or Buffer A contained 20uM non-hydrolyzable GTP. Wash buffer was Buffer A plus the addition of 25mM Imidazole. Elution buffer was Buffer A plus the addition of 300mM Imidazole.

To purify his-RAS proteins contained 3mL of amylose resin (New England BioLabs) was added to the column and EtOH solution was allowed to gravity drip to a final resin volume of 2mL. Buffer A contained 20uM GDP or Buffer A contained 20uM non-hydrolyzable GTP. The wash buffer for amylose resin, was the same as Buffer A. Elution buffer is Buffer A plus the addition of 10mM maltose.

The nickel resin beads were resuspended in the 50mL his-RAS sample solution and incubated, while rocking, at 4C for 1hr. The entire sample plus resin suspension was transferred back to the column and allowed to gravity filter. A 10uL sample from the flow through is taken (FT = flow through) and the remainder is discarded. The his-RAS sample plus resin was washed 2 times with 5mL of wash buffer. A 10uL sample from the flow through is taken (W1-2 = wash 1-2). For elution, the his-RAS sample plus resin is resuspended with 5mL of elution buffer and allowed to gravity filter. The 5mL elution samples are saved to confirm which samples contain the recombinant protein. A 10uL sample from the flow through was taken (E1 = elution sample 1). This is repeated 2 times and a 10uL sample from the flow through was taken (E2-3 = elution sample 2-3).

This process is the same for MBP-RAS recombinant proteins, using the appropriate buffer solutions as defined.

The samples taken during the purification process were incubated for 5min at 95C and run on an SDS-PAGE gel. The elution samples 1-3 that display the recombinant protein at the expected molecular weight were selected for buffer exchange/concentration.

Buffer exchange/concentration:

Buffer exchange/concentration was performed in a 50mL concentrator tube, by centrifugation using Buffer A until the Imidazole was removed from the sample. The elution samples that were shown to contain the recombinant protein were combined into the concentrator, and Buffer A was added until a final 50mL volume. The samples were centrifuged at 4000rmp for 15min at 4C. The flow through was discarded, and this process was repeated, as necessary. The ideal final target protein concentration was > 4mg/mL, with final volume 500uL as the minimal volume acceptable.

Protein concentration was determined using the molecular weight and extinction coefficient of the tagged recombinant protein.

Size exclusion chromatography:

Initially, each sample was filtered in a microcentrifuge column at 15,000rpm for 5min at 4C. Each size exclusion chromatography sample run contained a total of 250uL. For the mixed samples, his-KRAS and his-NRAS were mixed and incubated for 5min prior to centrifuge filtration; similarly, his-RAS and MBP-RAS were mixed and incubated prior to centrifuge filtration. Size exclusion chromatography was performed in the appropriate column at a flow rate of 1mL/min for a total of 30mL. Size exclusion chromatography with only his-RAS was performed on column with 70kDa maximum molecular weight size, with relevant standards. Size exclusion chromatography with his-RAS plus MBP-RAS was performed on column with 650kDa maximum molecular weight size, with relevant standards. Fractions were collected in unbiased method to subsequent reruns or SDS-PAGE analysis, as necessary.

BIBLIOGRAPHY

1 E Grabocka, Y Pylayeva-Gupta, MJK Jones, V Lubkov, E Yemanaberhan, L Taylor, HH Jeng, D Bar-Sagi. Wild-Type H- and N-Ras Promote Mutant K-Ras-Driven Transformation by Modulating the DNA Damage Response. *Cancer Cell* **25**, 243–256 (2014).

2 Network, The Cancer Genome Atlas Research. Comprehensive molecular profiling of lung adenocarcinoma. *Nature* **511**, 543–550, doi:10.1038/nature13385 (2014).

3 Z Zhang , Y Wang, HG Vikis, L Johnson, G Liu, J Li, MW Anderson, RC Sills, HL Hong, TR Devereux, T Jacks, K-L Gun, M You. Wildtype *Kras2* can inhibit lung carcinogenesis in mice. *Nature Genetics* **25**, 25-33, doi:10.1038:/ng721 (2001).

4 R Spencer-Smith, A Koike, Y Zhou, RR Eguchi, F Sha, P Gajwani, D Santana, A Gupta, M Jacobs, E Herrero-Garcia, J Cobbert, H Lavoie, M Smith, T Rajakulendran, E Dowdell, MN Okur, I Dementieva, F Sicheri, M Therrien, JF Hancock, M Ikura, S Koide, JP O'Bryan. Inhibition of RAS function through targeting an allosteric regulatory site. *Nat. Chem. Biol.* **13**, 62–68, doi:10.1038/nchembio.2231 (2017).

5 Network, The Cancer Genome Atlas Research. Integrated Genomic Characterization of Pancreatic Ductal Adenocarcinoma. *Cancer Cell* **32**, 185-203 (Integrated Genomic Characterization of Pancreatic Ductal Adenocarcinoma).

6 C Ambrogio, J Kohler, Z-W Zhou, H Wang, R Paranal, J Li, M Capelletti, C Caffarra, S Li, Q Lv, S Gondi, JC Hunter, J Lu, R Chiarle, D Santamaria, KD Westover, PA Janne KRAS Dimerization Impacts MEK Inhibitor Sensitivity and Oncogenic Activity of Mutant KRAS. *Cell* **172**, 857-868, doi:10.1016/j.cell.2017.12.020 (2018).

7 N Rizvi, MD Hellmann, A Snyder, P Kvistborg, V Makarov, JJ Havel, W Lee, J Yuan, P Wong, TS Ho, ML Miller, N Rekhtman, AL Moreira, F Ibrahim, C Bruggeman, B Gasmi, R Zappasodi, Y Maeda, C Sander, EB Garon, T Merghoub, JD Wolchok, TN Schumacher, TA Chan. Mutational lanscape determines sensitivity to PD-1 blockade in non-small cell lung cancer. *Science* **348**, 124-128 (2016).

8 JM Ostrem, U Peters, ML Sos, JA Wells, KM Shokat. K-Ras(G12C) inhibitors allosterically control GTP affinity and effector interactions. *Nature* **503**, 548-551, doi:doi:10.1038/nature12796 (2013).

9 Y Xiong, J Lu, J Hunter, L Li, D Scott, HG Choi, SM Lim, A Manandhar, S Gondi, T Sim, KD Westover, NS Gray. Covalent Guanosine Mimetic Inhibitors of G12C KRAS. *ACS medicinal chemistry letters* **8**, 61-66, doi:doi:10.1021/acsmedchemlett.6b00373 (2016).

10 Y Takai, T Sasaki, T Matozaki. Small GTP-Binding Proteins. *Physiological Reviews* **81**, 153-208, doi:10.1152/physrev.2001.81.1.153 (2001).

11 Barbacid, M. ras GENES. *Annual Review of Biochemistry* **56**, 779-827 (1987).

12 DK Simanshu, DV Nissley, F McCormick. RAS proteins and their regulators in human disease. *Cell* **170**, 17-33, doi:10.1016/j.cell.2017.06.009 (2017).

13 AM Waters, CJ Der KRAS: The Critical Driver and Therapeutic Target for Pancreatic Cancer. *Cold Spring Harbor perspectives in medicine* **8**, 1-23, doi:doi:10.1101/cshperspect.a031435 (2018).

14 NL Pershing, BL Lampson, JA Belsky, E Kaltenbrun, DM MacAlpine, CM Counter. Rare codons capacitate Kras-driven de novo tumorigenesis. *J Clin Invest* **125**, 222-233 (2015).

15 L Johnson, D Greenbaum, K Cichowski, K Mercer, E Murphy, E Schmitt, RT Bronson, H Umanoff, W Edelmann, R Kucherlapati, T Jacks. K-ras is an essential gene in the mouse with partial functional overlap with N-ras. *Genes & Development* **11**, 2468-2482 (1997).

16 L Gutierrez, AI Magee, CJ Marshall, JF Hancock. Post-translational processing of p2lras is two-step and involves carboxyl-methylation and carboxy-terminal proteolysis. *The EMBO Journal* **8**, 1093-1098 (1989).

17 JF Hancock, AI Magee, JE Childs, CJ Marshall. All ras proteins are polyisoprenylated but only some are palmitoylated. *Cell* **57**, 1167-1177 (1989).

18 JH Jackson, CG Cochrane, JR Bourne, PA Solski, JE Buss, CJ Der. Farnesol modification of Kirsten-ras exon 4B protein is essential for transformation. *Proc. Natl. Acad. Sci. USA* **87**, 3042-3046 (1990).

19 DB Whyte, P Kirschmeier, TN Hockenberry, I Nunez-Oliva, L James, JJ Catino, WR Bishop, J-K Pai. K- and N-Ras are Geranylgeranylated in Cells Treated with Farnesyl Protein Transferase Inhibitors. *Journal of Biological Chemistry* **22**, 14459-14464 (1997).

20 JC Wolfman, SM Planchon, J Liao, A Wolfman. Structural and functional consequences of c-N-Ras constitutively associated with intact mitochondria. *Biochim Biophys Acta* **1763**, 1108-1124 (2006).

21 CR Amendola, JP Mahaffey, SJ Parker, IM Ahearn, W-C Chen, M Zhou, H Court, J Shi, SL Mendoza, MJ Morten, E Rothenberg, E Gottlieb, YZ Wadghiri, R Possemato, SR Hubbard, A Balmain, AC Kimmelman, MR Phillips KRAS4A directly regulates hexokinase1. *Nature* **576**, 482-489, doi:10.1038/s41586-019-1832-9 (2019).

22 JL Bos, H Rehmann, A Wittinghofer. GEFs and GAPs: Critical Elements in the Control of Small G Proteins. *Cell* **129**, 865-877 (2007).

23 Aronheim, A. Membrane targeting of the nucleotide exchange factor Sos is sufficient for activating the Ras signaling pathway. *Cell* **78**, 949-961, doi:doi: 10.1016/0092-8674(94)90271-2 (1994).

24 S Jones, M-L Vignais, JR Broach. The *CDC25* Protein of *Saccharomyces cerevisiae* Promotes Exchange of Guanine Nucleotides Bound to Ras. *Molecular and Cellular Biology* **11**, 2641-2646 (1991).

25 SB Waters, KH Holt, SE Ross, L-J Syu, K-L Guan, JE Pessin. Desensitization of Ras Activation by a Feedback Disassociation of the SOS-Grb2 Complex. *J. Biol. Chem.* **270**, 20883-20886 (1995).

26 Stephen, AG. Dragging Ras Back in the Ring. *Cancer Cell* **25**, 272-281 (2014).

27 KM Haigis, KR Kendall, Y Wang, A Cheung, MC Haigis, JN Glickman, M Niwa-Kawakita, A Sweet-Cordero, J Sebolt-Leopold, KM Shannon, J Settleman, M Giovannini, T Jacks. Differential effects of oncogenic K-Ras and N-Ras on proliferation, differentiation and tumor progression in the colon. *Nature Genetics* **50**, 600-608 (2008).

28 M Malumbres, Mariano Barbacid. *RAS* oncogenes: the first 30 years. *Nature* **3**, 7-13 (2003).

29 BL Lampson, NLK Pershing, JA Prinz, JR Lacsina, WF Marzluff, CV Nicchitta, DM MacAlpine, CM Counter. Rare Codons Regulates KRas Oncogenesis. *Curr Biol.* **23**, 70-75, doi:10.1016/j.cub.2012.11.031 (2013).

30 J Hunter, A Manandhar, MA Carrasco, D Gurbani, S Gondi, KD Westover. Biochemical and Structural Analysis of Common Cancer-Associated KRAS Mutations. *Molecular Cancer Research* **13**, 1325 (2015).

31 M Drosten, A Dhawahir, EYM Sum, J Urosevic, CG Lechuga, LM Esteban, E Castellano, C Guerra, E Santos, M Barbacid. Genetic analysis of Ras signalling pathways in cell proliferation, migration and survival. *The EMBO Journal* **29**, 1091–1104, doi:doi:10.1038/emboj.2010.7 (2010).

32 Castellano, E. Requirement for interaction of PI3-kinase p110α with RAS in lung tumor maintenance. *Cancer Cell* **24**, 617630, doi:doi:10.1016/j.ccr.2013.09.012 (2013).

33 K Gottlob, N Majewski, S Kennedy, E Kandel, RB Robey, N Hay. Inhibition of early apoptotic events by Akt/PKB is dependent on the first committed step of glycolysis and mitochondrial hexokinase. *Genes & Development* **15**, 1406-1418, doi:10.1101/gad.889901 (2001).

34 VTHBM Smit, AJM Boot, AMM Smits, GJ Fleuren, CJ Cornelisse, JL Bos. KRAS codon 12 mutations occur very frequently in pancreatic adenocarcinoma. *Nucleic Acids Research* **16**, 7773-7782 (1988).

35 K Shimizu, D Birnbaum, MA Ruley, O Fasano, Y Suard, L Edlund, E Taparowsky, M Goldfarb, M Wigler. Structure of Ki-*ras* gene of the human lung carcinoma cell line Calu-1. *Nature* **304**, 497–500 (1983).

36 U Krengel, I Schlichting, A Scherer, R Schumann, M Frech, J John, W Kabsch, EF Pai, A Wittinghofer Three-Dimensional Structures of H-*ras* p21 Mutants: Molecular Basis for Their Inability to Function As Signal Switch Molecules. *Cell* **62**, 539-548 (1990).

37 L Tong, AM de Vos, MV Milburn, S-H Kims Crystal Structures at 2.2 A Resulution of the Catalytic Domains of Normal *ras* Protein and an Oncogenic Mutant Complexed with GDP. *J. Mol. Biol.* **217**, 503-516 (1991).

38 IA Prior, C Muncke, RG Parton, JF Hancock. Direct visualization of Ras proteins in spatially distinct cell surface microdomains. *J Cell Biol* **160**, 165-170, doi:10.1083/jcb.200209091 (2003).

39 SJ Plowman, C Muncke, RG Parton, JF Hancock. H-ras, K-ras, and inner plasma membrane raft proteins operate in nanoclusters with differential dependence on the actin cytoskeleton. *Proc Natl Acad Sci U S A* **102**, 15500-15505, doi:10.1073/pnas.0504114102 (2005).

40 D Abankwa, AA Gorfe, JF Hancock. Ras nanoclusters: molecular structure and assembly. *Semin Cell Dev Biol* **18**, 599-607, doi:10.1016/j.semcdb.2007.08.003. (2007).

41 X Nan, TM Tamguney, EA Collison, L-J Lin, C Pitt, J Galeas, S Lewis, JW Gray, F McCormick, S Chu. Ras-GTP dimers activate the Mitogen-Activated Protein Kinase (MAPK) pathway. *PNAS* **112**, 7996–8001, doi:10.1073/pnas.1509123112 (2015).

42 S Muratcioglu, TS Chavan, BC Freed, H Jang, L Khavrutskii, RN Freed, MA Dyba, K Stefanisko, SG Tarasov, A Gursoy, O Keskin, NI Tarasova, V Gaponenko, R Nussinov. GTP-Dependent K-Ras Dimerization. *Structure* **23**, 1325–1335, doi:10.1016/j.str.2015.04.019 (2015).

43 J Guldenhaupt, T Rudack, P Bachler, D Mann, G Triola, H Waldmann, C Kotting, K Gerwert. N-Ras Forms Dimers at POPC Membranes. *Biophysical Journal* **103**, 1585-1593 (2012).

44 D Abankwa, AA Gorfe, K Inder, JF Hancock. Ras membrane orientation and nanodomain localization generate isoform diversity. *PNAS* **103**, 1130–1135, doi:10.1073/pnas.0903907107 (2010).

45 TG Bivona, SE Quatela, BO Bodemann, IM Ahearn, MJ Soskis, A Mor, J Miura, HH Weiner, L Wright, SG Saba, D Yim, A Fein, IP de Castro, C Li, CB Thompson, AD Cox.

PKC Regulates a Farnesyl-Electrostatic Switch on K-Ras that Promotes its Association with Bcl-XL on Mitochondria and Induces Apoptosis. *Molecular Cell* **21**, 481-493 (2006).

46 TD Martin, DR Cook, MY Choi, MZ Li, KM Haigis, SJ Elledge. A Role for Mitochondrial Translation in Promotion of Viability in K-Ras Mutant Cells. *Cell Reports* **20**, 427-438 (2017).

47 Omidvar, Nader. BCL-2 and Mutant NRAS Interact Physically and Functionally in a Mouse Model of Progressive Myelodysplasia. *Cancer Research* **67**, 11657-11667 (2007).

48 C-HJ Lee, NG Della, CE Chew, DJ Zack Rin, a neuron-specific and calmodulin-binding small G-protein, and Rit define a novel subfamily of Ras proteins. *Journal of Neuroscience* **16**, 6784-6794 (1996).

49 H Shao, K Kadono-Okuda, BS Finlin, DA Andres. Biochemical characterization of the Ras-related GTPases Rit and Rin. *Archives of Biochemistry and Biophysics* **371**, 207-219 (1999).

50 G-X Shi, W Cai, DA Andres. Rit subfamily small GTPases: Regulators in nueronal differentiation and survivial. *Cell Signal* **25**, 2060-2068, doi:10.1016/j.cellsig.2013.06.002 (2013).

51 Z Fang, CB Marshall, JC Yin, MT Mazhab-Jafari, GMC Gasmi-Seabrook, MJ Smith, T Nishikawa, Y Xu, BG Neel, M Ikura. Biochemical classification of disease-associated mutants of RAS-like protein expressed in many tissues (RIT1). *Journal of Biological Chemistry* **291**, 15641-15652, doi:10.1074/jbc.M116.714196 (2016).

52 P Castel, A Cuevas-Navarro, DB Everman, AG Papageorge, DK Simanshu, A Tankka, J Galeas, A Urisman, F McCormick. RIT1 oncoproteins escape LZTR1-mediated proteolysis. *Science* **363**, 1226-1229, doi:10.1126/science.aav1444 (2019).

53 M Hoshino, T Yoshimori, S Nakamura. Small GTPase proteins Rin and Rit bind to PAR6 GTP-dependently and regulate cell transformation. *Journal of Biological Chemistry* **280**, 22868-22874 (2005).

54 MB Menon, M Gaestel. MK2–TNF–Signaling Comes Full Circle. *Trends Biochem Sci* **43**, 170-179, doi:10.1016/j.tibs.2017.12.002 (2018).

55 I Cirstea, K Kutsche, R Dvorsky, L Gremer, C Carta, D Horn, AE Roberts, F Lepri, . A restricted spectrum of *NRAS* mutations causes Noonan syndrome. *Nature Genetics* **42**, 27-29, doi:10.1038/ng.497 (2010).

56 S Schubbert, M Zenker, SL Rowe, S Boll, C Klein, G Bollag, I van der Burgt, L Musante, V Kalscheuer, L-E Wehner, H Nguyen, B West, KYJ Zhang, E Sistermans, A Rauch, CM Niemeyer, K Shannon, CP Kratz. Germline KRAS mutations cause Noonan syndrome. *Nature Genetics* **38**, 331-336, doi:10.1038/ng1748 (2006).

57 Y Aoki, T Niihori, T Banjo, N Okamoto, S Mizuno, K Kurosawa, T Ogata, F Takada, M Yano, T Ando, T Hoshika, C Barnett, H Ohashi, H Kawame, T Hasegawa, T Okutani, T Nagashima, S Hasegawa, R Funayama, T Nagashima, K Nakayama, S-i Inoue, Y Watanabe, T Ogura, Y Matsubara. Gain-of-function mutations in *RIT1* cause Noonan Syndrome, a RAS/MAPK pathway syndrome. *The American Journal of Human Genetics* **93**, 173-180 (2013).

58 A Estep, WE Tidyman, MA Teitell, PD Cotter, KA Rauen. HRAS mutations in Costello Syndrome: Detetion of constitutional activating mutations in codon 12 and 13 and loss of wild-type allele in malignancy. *American Journal of Medical Genetics* **140A**, 8-16, doi:10.1002/ajmg.a.31078 (2006).

59 AA Romano, JE Allanson, JD Dahlgren, BD Gelb, B Hall, ME Pierpont, AE Roberts, W Robinson, CM Takemoto, JA Noonan. Noonan syndrome: Clinical features, diagnosis, and management guidelines. *Pediatrics* **126**, 746-759 (2010).

60 Der, A Waters & CJ. KRAS: The critical driver and therapeutic target for pancreatic cancer. *Cold Spring Harbor Perspect Med* 1-23, doi:10.1101/cshperspect.a031435 (2017).

61 SA Forbes, N Bindal, S Bamford, C Cole, CY Kok, D Beare, M Jia, R Shepherd, K Leung, A Menzies, JW Teague, PJ Campbell, MR Stratton, PA Futreal. COSMIC: mining complete cancer genomes in the Catalogue of Somatic Mutations in Cancer. **39**, D945-D950 (2011).

62 S Li, A Balmain, CM Counter. A model for RAS mutation patterns in cancers: finding the sweet spot. *Nat Rev Cancer* **18**, 767-777, doi:10.1038/s41568-018-0076-6 (2018).

63 M Sanchez-Cespedes, SA Ahrendt, S Piantadosi, R Rosell, M Monzo, L Wu, WH Westra, SC Yang, J Jen, D Sidransky. Chromosomal Alterations in Lung Adenocarcinoma from Smokers and Nonsmokers. *Cancer Research*, 1309-1313 (2001).

64 MD To, R Del Rosario, PMK Westcott, KL Banta, A Balmain. Interactions Between Wildtype and Mutant *Ras* Genes in Lung and Skin Carcinognesis. *Oncogene* **32**, 4028–4033, doi:10.1038/onc.2012.404 (2013).

65 AH Berger, M Imielinski, F Duke, J Wala, N Kaplan, G-X Shi, DA Andres, M Myerson. Oncogenic RIT1 mutations in lung adenocarcinoma. *Oncogene* **33**, 4418-4423 (2014).

66 A Vichas, NT Nkinsi, A Riley, PCR Parrish, F Duke, J Chen, I Fung, J Watson, M Rees, JK Lee, F Piccioni, EM Hatch, AH Berger, Alice H. An integrative oncogene-dependency map identifies unique vulnerabilities of oncogenic EGFR, KRAS, and RIT1 in lung cancer. *bioRxiv*, 2020.2007.2003.187310, doi:10.1101/2020.07.03.187310 (2020).

67 A Krystiniak, C Garcia-Echeverria, C Prigent, S Ferrari. Inhibition of Aurora A in response to DNA damage. *Oncogene* **25**, 338-348 (2006).

68 Mok, TS. Gefitinib or carboplatin-paclitaxel in pulmonary adenocarcinoma. *N Engl J Med* **361**, 947–957 (2009).

69 Paez, JG. EGFR mutations in lung cancer: correlation with clinical response to gefitinib therapy. *Science* **304**, 1497-1500, doi:doi:10.1126/science.1099314 (2004).

70 M Holderfield, MM Deuker, F McCormick, M McMahon. Targeting RAF kinases for cancer therapy: BRAF mutated melanoma and beyond. *Nat Rev Cancer* **14**, 455-467, doi:10.1038/nrc3760 (2014).

71 SJ Heidorn, C Milagre, S Whittaker, A Nourry, I Niculescu-Duvas, N Dhomen, J Hussain, JS Reis-Filho, CJ Springer, C Pritchard, R Marais. Kinase-dead BRAF and oncogenic RAS oncogenic RAS cooperate to drive tumor progression through CRAF. *Cell* **140**, 209-221 (2015).

72 G Hatzivassiliou, K Song, I Yen, BJ Brandhuber, DJ Anderson, R Alvarado, MJC Ludlam, D Stokoe, SL Gloor, G Vigers, T Morales, I Aliagas, B Liu, S Sideris, KP Hoeflich, BS Jaiswal, S Seshagiri, H Koeppen, M Belvin, LS Friedman, S Malek. RAF inhibitors prime wild-type RAF to activate the MAPK pathway and enhance growth. *Nature* **464**, 431-435 (2010).

73 PI Poulikakos, C Zhang, G Bollag, KM Shokat, N Rosen. RAF inhibitors transactivate RAF dimers and ERK signaling in cells with wild-type BRAF. *Nature* **464**, 427-430 (2010).

74 KA Arkhipova, AN Sheyderman, KK Laktionov, VV Mochalnikova, IB Zborovskaya. Simultaneous expression of flotillin-1, flotillin-2, stomatin and caveolin-1 in non-small cell lung cancer and soft tissue sarcomas. *BMC Cancer* **14: 100**, 1-9, doi:10.1186/1471-2407-14-100 (2014).

75 U Salzer, M Mairhofer, R Prohaska. *Stomatin: A New Paradigm of Membrane Organization Emerges*. Vol. 1 20-33 (2007).

76 L Snyers, E Umlauf, R Prohaska. Oligomeric Nature of the Integral Membrane Protein Stomatin. *Journal of Biological Chemistry* **273**, 17221-17226 (1998).

77 MF Baietti, M Simicek, LA Asbagh, E Radaelli, S Lievens, J Crowther, M Steklov, VN Aushev, D M Garcia, J Tavernier, AA Sablina. OTUB1 triggers lung cancer development by inhibiting RAS monoubiquitination. *EMBO Molecular Medicine* **8(3)**, 288-303 (2016).

78 N Shindo-Okada, K Takeuchi, B-S Han, Y Nagamachi. Establishment of Cell Lines with High and Low Metastatic Potential from A549 Human Lung Adenocarcinoma. *Jpn. J. Cancer Res.* **93**, 50-60 (2002).

79 Singh, A. A gene expression signature associated with 'K-Ras addiction' reveals regulators of EMT and tumor cell survival. *Cancer Cell* **15**, 489-500 (2009).

80 X Ye, RA Weinberg. Epithelial-Mesenchymal Plasticity: A central regulator of cancer progression. *Trends Cell Biol.* **25(11)**, 675-686 (2015).

81 J Bartek, J Bartkova, J Taylor-Papadimitriou, A Rejthar, J Kovarik, Z Lukas, B Vojtesek. Differential expression of keratin 19 in normal human epithelial tissues revealed by monospecific monoclonal antibodies. *Histochemical Journal* **18**, 565-575 (1986).

82 YW Moon, G Rao, JJ Kim, H-S Shim, K-S Park, SS An, B Kim, PS Steeg, S Sarfaraz, L Changwoo Lee, D Voeller, EY Choi, J Luo, D Palmieri, HC Chung, J-H Kim, Y Wang, G Giaccone. LAMC2 enhances the metastatic potential of lung adenocarcinoma. *Cell Death and Differentiation* **22**, 1341-1352 (2015).

83 Gettinger, S. Impaired HLA Class I Antigen Processing and Presentation as a Mechanismof Acquired Resistance to Immune Checkpoint Inhibitors in Lung Cancer. *Cancer Discov.* **7**, 1420-1435 (2017).

84 Seliger, B. Down-regulation of the MHC class I antigen-processing machinery after oncogenic transformation of murine fibroblasts. *Eur. J. Immunol.* **28**, 122-133 (1998).

85 M-S Mo, W Huang, C-C Sun, L-M Zhang, L Cen, Y-S Xiao, G-F Li, X-L Yang, S-G Qu, P-Y Xu. Association Analysis of Proteasome Subunits and Transporter Associated with Antigen Processing on Chinese Patients with Parkinson's Disease. *Chinese Medical Journal* **129** (2016).

86 Pylayeva-Gupta, Y. RAS oncogenes: weaving a tumorigenic web. *Nat. Rev. Cancer* **11**, 761-774 (2006).

87 JE Mirus, Y Zhang, CI Li, AE Lokshin, RL Prentice, SR Hingorani, PD Lampe. Cross-species antibody microarray interrogation identifies a 3- protein panel of plasma biomarkers for early diagnosis of pancreas cancer. *Clin Cancer Res* **21**, 1764-1771, doi:10.1158/1078-0432.CCR-13-3474 (2015).

VITA

My overall research interest is in precision medicine and identifying therapeutically opportunities based upon the genetic perturbations underlying the disease. My academic training and research have given me a fundamental background in the fields of biomedical engineering, molecular biology, and genome engineering. After receiving my B.S. in biomedical engineering, I transitioned to the fast-paced world of a biotech manufacturing company in San Diego county, with roles in Quality Assurance at Aalto Scientific, Ltd. Seeking a deeper understanding of the transition between research and manufacturing, I joined the Process Development (scale up) department at the start-up, Marrone BioInnovations, Inc. located in Davis, CA. My biotech experience working in commercial labs has allowed me to beneficially bring industry standards to my academic research. I completed the Master of Science in Molecular and Cell Biology with an emphasis in Stem Cell Biology program at San Francisco State University in May 2016. As a student in this program, I completed my thesis project at the Gladstone Institute of Cardiovascular Disease. While at Gladstone, my research used CRISPR gene-editing of human induced pluripotent stem cells to model cardiomyopathy. In order to foster and gain experience in scientific communication, I presented a poster at the 15th Annual Biomedical Research Conference for Minority Students (ABRCMS). ABRCMS 2015 was held in Seattle, WA, Nov 11-14, 2015. My poster was entitled, "Tracking RBM20-Induced Cardiomyopathy in human iPS-Cardiomyocytes." While at University of Washington I have continued my interest in precision to understand the mechanism and targeting of cancer 'driver' genes, in order to translate this information into clinical benefits to patients. I was awarded a travel award to attend the 5th AACR-IASLC Joint Conference: Lung Cancer Translational Science from the Bench to the Clinic, and present my poster entitled "Differential sensitivity to Aurora kinase inhibition in *RIT1*- and *KRAS*-mutant lung adenocarcinoma." Continuing this theme, my current research will determine if Ras family members heterodimerize, and if this presents a therapeutic opportunity to treat *KRAS*-mutant lung adenocarcinoma. Additional research at the Fred Hutch Cancer Research Center identified similar and different functions of RIT1 and KRAS proteome in lung adenocarcinoma. After earning a PhD at the University of Washington, I hope to continue doing research in the biotechnology/pharmaceutical industry.